

# Water Resources Research

AN AGU JOURNAL

**Aims and Scope.** *Water Resources Research* is an interdisciplinary journal that publishes original research in the natural and social sciences of water. This includes the role of water in the physical, chemical, biological, and ecological sciences; public health; and related social and policy sciences. It encompasses methodological development of observational, experimental, theoretical, analytical, numerical, and data driven approaches that advance the science of water and its management. Submissions are evaluated for their novelty, accuracy, significance, and broader implications of the findings.

**Editors:** Alberto Montanari (Editor in Chief) ([alberto.montanari@unibo.it](mailto:alberto.montanari@unibo.it)), Jean Bahr (<http://orcid.org/0000-0001-5500-3477>), Günter Blöschl, Ximing Cai, D. Scott Mackay (<http://orcid.org/0000-0003-0477-9755>), Anna Michalak, Harihar Rajaram, Xavier Sanchez-Vila.

**Associate Editors:** Kumud Acharya, Christophe Ancey, Shmuel Assouline, Alberto Bellin, M.F.P. Bierkens, Andrew Binley, William Blomquist, Fulvio Boano, Casey Brown, Attilio Castellarin, Andrea Castelletti, Sudeep Chandra, Olaf Cirpka, Martyn Clark, Miriam Coenders, Francesco Comiti, Russell Detwiler, Joshua Duke, Diane Dupont, Amin Elshorbagy, Brent Ewers, Steven Fassnacht, Daniel Fernandez-Garcia, Mario J. França, Michael Gooseff, Jonathan Gourley, Alberto Guadagnini, Rainer Helmig, Catherine Heppell, Erich Hester, Markus Hilpert, Sander Huisman, Erkan Istanbuluoglu, Zoran Kapelan, Christopher Keylock, Anton Kruger, Francesco Laio, Andreas Langousis, Laura K. Lutz, Xu Liang, Gaisheng Liu, Di Long, Charlie Luce, Jessica Lundquist, Jennifer McIntosh, Holly Michael, Burke Minsley, Noah Molotch, Dan Moore, Hamid Moradkhani, Stephen Moyses, Larry Murdoch, Guo-Yue Niu, Jan Martin Nordbotten, Denis O'Carroll, Sheila M. Olmstead, Stefano Orlandini, Thanos Papanicolaou, Shirley Papuga, Juraj Parajka, Valentijn Pauwels, Dubravka Pokrajac, Manuel Pulido-Velazquez, Patrick Reed, Benjamin Renard, Dieter Rickenmann, Monica Riva, Magdalena Rogger, Kevin Christopher Rose, David Rupp, Nick Rutter, Patricia Saco, Luis Samaniego, Bridget R. Scanlon, Marcel G. Schaap, Rina Schumer, Gerardo Severino, Kamini Singha, Lee Slater, Daniel Tartakovsky, Christoph Thomas, Tetsu K. Tokunaga, Daniele Tonina, V. Venugopal, Alberto Viglione, Ann Michelle Walvoord, Andrew Western, Bradford Wilcox, Alicia Wilson, Fu-Chun Wu, Ming Ye.

**AGU Editorial Team.** For assistance with submitted manuscripts, file specifications, or AGU publication policy please contact [wrr@agu.org](mailto:wrr@agu.org).

For submission instructions or to submit a manuscript visit: <http://wrr-submit.agu.org/>.

The journal to which you are submitting your manuscript employs a plagiarism detection system. By submitting your manuscript to this journal you accept that your manuscript may be screened for plagiarism against previously published works.

*Water Resources Research* accepts articles for Open Access publication. Please visit <http://olabout.wiley.com/WileyCDA/Section/id-406241.html> for further information about OnlineOpen.

**Publication Charges.** The publication charge income received for *Water Resources Research* helps support rapid publication, allows more articles per volume, makes possible the low subscription rates, and supports many of AGU's scientific and outreach activities. Publication charge information can be found here: <http://publications.agu.org/author-resource-center/publication-fees/>.

To encourage papers to be written in a concise fashion, there is an excess length fee. For *Water Resources Research*, the fee is assessed only on the equivalent of more than 25 publication units. The excess length fee does not apply to review articles, and the editor may waive the fee on a limited number of concisely written papers that merit being longer. There is no charge for color in any format.

**Copyright and Photocopying.** Copyright © 2016. American Geophysical Union. All rights reserved. No part of this publication may be reproduced, stored or transmitted in any form or by any means without the prior permission in writing from the copyright holder. Authorization to copy items for internal and personal use is granted by the copyright holder for libraries and other users registered with their local Reproduction Rights Organisation (RRO), e.g.

Copyright Clearance Center (CCC), 222 Rosewood Drive, Danvers, MA 01923, USA ([www.copyright.com](http://www.copyright.com)), provided the appropriate fee is paid directly to the RRO. This consent does not extend to other kinds of copying such as copying for general distribution, for advertising or promotional purposes, for creating new collective works or for resale. Special requests should be addressed to: [publications@agu.org](mailto:publications@agu.org).

**Disclaimer.** The Publisher, American Geophysical Union, and Editors cannot be held responsible for errors or any consequences arising from the use of information contained in this journal; the views and opinions expressed do not necessarily reflect those of the Publisher, American Geophysical Union, and Editors, neither does the publication of advertisements constitute any endorsement by the Publisher, American Geophysical Union, and Editors of the products advertised.

**Individual Subscriptions.** Member subscriptions are available through [members.agu.org](http://members.agu.org) or by contacting the AGU Member Service Center. The Service Center is open from 8:00 a.m. to 8:30 p.m. Eastern time: +1 202 462 6900, +1 800 966 2481; Fax: +1 202 777 7393; e-mail: [service@agu.org](mailto:service@agu.org). Questions about meetings or membership will be referred to the appropriate staff.

**Publisher.** *Water Resources Research* is published on behalf of the American Geophysical Union by Wiley Periodicals, Inc., 111 River St., Hoboken, NJ, 07030-5774, +1 201 748 6000.

**Delivery Terms and Legal Title.** Where the subscription price includes print issues and delivery is to the recipient's address, delivery terms are Delivered at Place (DAP); the recipient is responsible for paying any import duty or taxes. Title to all issues transfers FOB our shipping point, freight prepaid. We will endeavour to fulfil claims for missing or damaged copies within six months of publication, within our reasonable discretion and subject to availability.

*WATER RESOURCES RESEARCH* (ISSN 0043-1397), is published monthly by Wiley Subscription Services, Inc., a Wiley Company, 111 River St., Hoboken, NJ 07030-5774.

Periodicals Postage Paid at Hoboken, NJ and additional offices.

Postmaster: Send all address changes to *WATER RESOURCES RESEARCH*, John Wiley & Sons Inc., C/O The Sheridan Press, PO Box 465, Hanover, PA 17331.

**Journal Customer Services.** For institutional subscription information, claims and any enquiry concerning your journal subscription please go to [www.wileycustomerhelp.com/ask](http://www.wileycustomerhelp.com/ask) or contact your nearest office.

**Americas:** Email: [cs-journals@wiley.com](mailto:cs-journals@wiley.com); Tel: +1 781 388 8598 or +1 800 835 6770 (toll free in the USA & Canada).

**Europe, Middle East and Africa:** Email: [cs-journals@wiley.com](mailto:cs-journals@wiley.com); Tel: +44 (0) 1865 778315.

**Asia Pacific:** Email: [cs-journals@wiley.com](mailto:cs-journals@wiley.com); Tel: +65 6511 8000.

**Japan:** For Japanese speaking support, Email: [cs-japan@wiley.com](mailto:cs-japan@wiley.com); Tel: +65 6511 8010 or Tel (toll-free): 005 316 50 480.

Visit our Online Customer Help available in 7 languages at [www.wileycustomerhelp.com/ask](http://www.wileycustomerhelp.com/ask).

**Production Editor.** For assistance with post-acceptance articles and other production issues, please contact [wrcrprod@wiley.com](mailto:wrcrprod@wiley.com).

Access to this journal is available free online within institutions in the developing world through the AGORA initiative with the FAO, the HINARI initiative with the WHO, the OARE initiative with UNEP, and the ARDI initiative with WIPO. For information, visit [www.aginternetwork.org](http://www.aginternetwork.org), [www.who.int/hinari/en/](http://www.who.int/hinari/en/), [www.oaresciences.org](http://www.oaresciences.org), or [www.wipo.int/ardi/en](http://www.wipo.int/ardi/en).

ISSN 0043-1397 (Print)  
ISSN 1944-7973 (Online)

View this journal online at <http://wrr.agu.org>.

**Cover.** From Figure 1 of Fuller et al. [DOI: 10.1002/2015WR017992]: Schematic drawing of the major components of a typical RoR project in B.C., Canada, including the primary sediment storage element (i.e. the head-pond). See pp. 2770–2788.

**Editorial**

- 2380** *Alberto Montanari, Jean Bahr, Günter Blöschl, Ximing Cai, D. Scott Mackay, Anna Michalak, Harihar Rajaram, and Xavier Sanchez-Vila*  
Appreciation of peer reviewers for 2015 (doi 10.1002/2016WR018922)
- 2399** *Demetris Koutsoyiannis, Günter Blöschl, András Bárdossy, Christophe Cudennec, Denis Hughes, Alberto Montanari, Insa Neuweiler, and Hubert Savenije*  
Joint editorial: Fostering innovation and improving impact assessment for journal publications in hydrology (doi 10.1002/2016WR018895)

**Research Articles**

- 2403** *E. Creaco, L. Berardi, Siao Sun, O. Giustolisi, and D. Savic*  
Selection of relevant input variables in storm water quality modeling by multiobjective evolutionary polynomial regression paradigm (doi 10.1002/2015WR017971)
- 2420** *H. Roshan, M. S. Andersen, H. Rutledge, C. E. Marjo, and R. I. Acworth*  
Investigation of the kinetics of water uptake into partially saturated shales (doi 10.1002/2015WR017786)
- 2439** *Matthew G. Bonnema, Safat Sikder, Faisal Hossain, Michael Durand, Colin J. Gleason, and David M. Bjerklie*  
Benchmarking wide swath altimetry-based river discharge estimation algorithms for the Ganges river system (doi 10.1002/2015WR017296)
- 2462** *Yong Zhang, Mark M. Meerschaert, and Roseanna M. Neupauer*  
Backward fractional advection dispersion model for contaminant source prediction (doi 10.1002/2015WR018515)
- 2474** *L. Stoeckl, M. Walther, and T. Graf*  
A new numerical benchmark of a freshwater lens (doi 10.1002/2015WR017989)
- 2490** *Chengzhong Pan, Lan Ma, John Wainwright, and Zhouping Shangguan*  
Overland flow resistances on varying slope gradients and partitioning on grassed slopes under simulated rainfall (doi 10.1002/2015WR018035)
- 2513** *Rui Hui, Elizabeth Jachens, and Jay Lund*  
Risk-based planning analysis for a single levee (doi 10.1002/2014WR016478)
- 2529** *Yuehao Tang, Qinghui Jiang, and Chuangbing Zhou*  
Approximate analytical solution to the Boussinesq equation with a sloping water-land boundary (doi 10.1002/2015WR017794)
- 2551** *Edom Moges, Yonas Demissie, and Hong-Yi Li*  
Hierarchical mixture of experts and diagnostic modeling approach to reduce hydrologic model structural uncertainty (doi 10.1002/2015WR018266)
- 2571** *Ian C. Tse, Cristina M. Poindexter, and Evan A. Variano*  
Wind-driven water motions in wetlands with emergent vegetation (doi 10.1002/2015WR017277)
- 2582** *Gonzalo Cortés, Manuela Giroto, and Steven Margulis*  
Snow process estimation over the extratropical Andes using a data assimilation framework integrating MERRA data and Landsat imagery (doi 10.1002/2015WR018376)
- 2601** *Amanda L. Dye, James E. McClure, David Adalsteinsson, and Cass T. Miller*  
An adaptive lattice Boltzmann scheme for modeling two-fluid-phase flow in porous medium systems (doi 10.1002/2015WR018279)
- 2618** *D. W. Vasco, Steven R. Pride, and Michael Commer*  
Trajectory-based modeling of fluid transport in a medium with smoothly varying heterogeneity (doi 10.1002/2015WR017646)
- 2647** *Guillaume Gianni, Julien Richon, Pierre Perrochet, Alexandre Vogel, and Philip Brunner*  
Rapid identification of transience in streambed conductance by inversion of floodwave responses (doi 10.1002/2015WR017154)
- 2659** *Andreas Langousis, Antonios Mamalakis, Michelangelo Puliga, and Roberto Deidda*  
Threshold detection for the generalized Pareto distribution: Review of representative methods and application to the NOAA NCDC daily rainfall database (doi 10.1002/2015WR018502)
- 2682** *Andrew W. Woods and Simon Norris*  
Dispersion and dissolution of a buoyancy driven gas plume in a layered permeable rock (doi 10.1002/2015WR018159)
- 2698** *Richard R. Rushforth and Benjamin L. Ruddell*  
The vulnerability and resilience of a city's water footprint: The case of Flagstaff, Arizona, USA (doi 10.1002/2015WR018006)
- 2715** *J. G. Venditti, M. Church, M. E. Attard, and D. Haught*  
Use of ADCPs for suspended sediment transport monitoring: An empirical approach (doi 10.1002/2015WR017348)
- 2737** *Leila Farhadi, Dara Entekhabi, and Guido Salvucci*  
Mapping land water and energy balance relations through conditional sampling of remote sensing estimates of atmospheric forcing and surface states (doi 10.1002/2015WR017680)

- 2753** *Philippe Naveau, Raphael Huser, Pierre Ribereau, and Alexis Hannart*  
Modeling jointly low, moderate, and heavy rainfall intensities without a threshold selection (doi 10.1002/2015WR018552)
- 2770** *Theodore K. Fuller, Jeremy G. Venditti, Peter A. Nelson, and Wendy J. Palen*  
Modeling grain size adjustments in the downstream reach following run-of-river development (doi 10.1002/2015WR017992)
- 2789** *Niannian Fan, Arvind Singh, Michele Guala, Efi Foufoula-Georgiou, and Baosheng Wu*  
Exploring a semimechanistic episodic Langevin model for bed load transport: Emergence of normal and anomalous advection and diffusion regimes (doi 10.1002/2015WR018023)
- 2802** *Christian Noss and Andreas Lorke*  
Roughness, resistance, and dispersion: Relationships in small streams (doi 10.1002/2015WR017449)
- 2822** *S. Mažeika P. Sullivan, Lindsey E. Boaz, and Katie Hossler*  
Fluvial geomorphology and aquatic-to-terrestrial Hg export are weakly coupled in small urban streams of Columbus, Ohio (doi 10.1002/2015WR018416)
- 2840** *Naomi S. Wells, W. Troy Baisden, Travis Horton, and Tim J. Clough*  
Spatial and temporal variations in nitrogen export from a New Zealand pastoral catchment revealed by stream water nitrate isotopic composition (doi 10.1002/2015WR017642)
- 2855** *Victor I. Malkovsky and Fabien Magri*  
Thermal convection of temperature-dependent viscous fluids within three-dimensional faulted geothermal systems: Estimation from linear and numerical analyses (doi 10.1002/2015WR018001)
- 2868** *Mark R. Williams, Kevin W. King, William Ford, Anthony R. Buda, and Casey D. Kennedy*  
Effect of tillage on macropore flow and phosphorus transport to tile drains (doi 10.1002/2015WR017650)
- 2883** *Michelle E. Newcomer, Susan S. Hubbard, Jan H. Fleckenstein, Ulrich Maier, Christian Schmidt, Martin Thullner, Craig Ulrich, Nicolas Flipo, and Yoram Rubin*  
Simulating bioclogging effects on dynamic riverbed permeability and infiltration (doi 10.1002/2015WR018351)
- 2901** *Alessio Domeneghetti*  
On the use of SRTM and altimetry data for flood modeling in data-sparse regions (doi 10.1002/2015WR017967)
- 2919** *S. M. Jepsen, T. C. Harmon, and Y. Shi*  
Watershed model calibration to the base flow recession curve with and without evapotranspiration effects (doi 10.1002/2015WR017827)
- 2934** *R. Vesipa, C. Camporeale, and L. Ridolfi*  
Recovery times of riparian vegetation (doi 10.1002/2015WR018490)
- 2951** *Christine J. Kirchhoff and Lisa Dilling*  
The role of U.S. states in facilitating effective water governance under stress and change (doi 10.1002/2015WR018431)
- 2965** *Jun Kong, Chengji Shen, Zhaoyang Luo, Guofen Hua, and Hongjun Zhao*  
Improvement of the hillslope-storage Boussinesq model by considering lateral flow in the unsaturated zone (doi 10.1002/2015WR018054)
- 2985** *Javier Benítez-Buelga, Leonor Rodríguez-Sinobas, Raul Sánchez Calvo, María Gil-Rodríguez, Chadi Sayde, and John S. Selker*  
Calibration of soil moisture sensing with subsurface heated fiber optics using numerical simulation (doi 10.1002/2015WR017897)
- 2996** *Neil Terry, Lee Slater, Xavier Comas, Andrew S. Reeve, Karina V. R. Schäfer, and Zhongjie Yu*  
Free phase gas processes in a northern peatland inferred from autonomous field-scale resistivity imaging (doi 10.1002/2015WR018111)
- 3019** *Mijanur R. Chowdhury, Mathew G. Wells, and Todd Howell*  
Movements of the thermocline lead to high variability in benthic mixing in the nearshore of a large lake (doi 10.1002/2015WR017725)
- 3040** *Olivia M. Stoken, Ami L. Riscassi, and Todd M. Scanlon*  
Association of dissolved mercury with dissolved organic carbon in U.S. rivers and streams: The role of watershed soil organic carbon (doi 10.1002/2015WR017849)
- 3052** *D. Jaskierniak, G. Kuczera, and R. Benyon*  
Predicting long-term streamflow variability in moist eucalypt forests using forest growth models and a sapwood area index (doi 10.1002/2015WR018029)
- 3068** *J. R. Lamontagne, J. R. Stedinger, Xin Yu, C. A. Whealton, and Ziyao Xu*  
Robust flood frequency analysis: Performance of EMA with multiple Grubbs-Beck outlier tests (doi 10.1002/2015WR018093)
- 3085** *Guilherme J. C. Gomes, Jasper A. Vrugt, and Eurípedes A. Vargas Jr.*  
Toward improved prediction of the bedrock depth underneath hillslopes: Bayesian inference of the bottom-up control hypothesis using high-resolution topographic data (doi 10.1002/2015WR018147)
- 3113** *Vincent Allègre, Emily E. Brodsky, Lian Xue, Stephanie M. Nale, Beth L. Parker, and John A. Cherry*  
Using earth-tide induced water pressure changes to measure in situ permeability: A comparison with long-term pumping tests (doi 10.1002/2015WR017346)
- 3127** *Sanjiv Kumar, Francis Zwiers, Paul A. Dirmeyer, David M. Lawrence, Rajesh Shrestha, and Arelia T. Werner*  
Terrestrial contribution to the heterogeneity in hydrological changes under global warming (doi 10.1002/2016WR018607)
- 3143** *Colin A. Penn, Lindsay A. Bearup, Reed M. Maxwell, and David W. Clow*  
Numerical experiments to explain multiscale hydrological responses to mountain pine beetle tree mortality in a headwater watershed\* (doi 10.1002/2015WR018300)

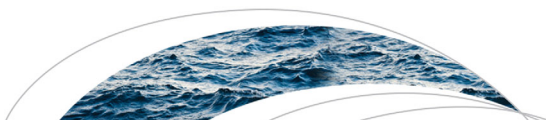
\*This article is part of a Special Section—Disturbance Hydrology

- 3162** *Dario Del Giudice, Carlo Albert, Jörg Rieckermann, and Peter Reichert*  
Describing the catchment-averaged precipitation as a stochastic process improves parameter and input estimation (doi 10.1002/2015WR017871)
- 3187** *Sven Wagner, Benjamin Fersch, Fei Yuan, Zhongbo Yu, and Harald Kunstmann*  
Fully coupled atmospheric-hydrological modeling at regional and long-term scales: Development, application, and analysis of WRF-HMS (doi 10.1002/2015WR018185)
- 3212** *Julia Wester, Kiara R. Timpano, Demet Çek, and Kenneth Broad*  
The psychology of recycled water: Factors predicting disgust and willingness to use (doi 10.1002/2015WR018340)
- 3227** *Noah M. Schmadel, Adam S. Ward, Marie J. Kurz, Jan H. Fleckenstein, Jay P. Zarnetske, David M. Hannah, Theresa Blume, Michael Vieweg, Phillip J. Blaen, Christian Schmidt, Julia L.A. Knapp, Megan J. Klaar, Paul Romeijn, Thibault Datry, Toralf Keller, Silvia Folegot, Amaia I. Marruedo Arricibita, and Stefan Krause*  
Stream solute tracer timescales changing with discharge and reach length confound process interpretation (doi 10.1002/2015WR018062)
- 3246** *Shengjie Wang, Mingjun Zhang, Yanjun Che, Fenli Chen, and Fang Qiang*  
Contribution of recycled moisture to precipitation in oases of arid central Asia: A stable isotope approach (doi 10.1002/2015WR018135)
- 3258** *Nataliya Le Vine*  
Combining information from multiple flood projections in a hierarchical Bayesian framework (doi 10.1002/2015WR018143)

**Technical Reports: Data**

- 3276** *Fiachra E. O'Loughlin, Jeffrey Neal, Dai Yamazaki, and Paul D. Bates*  
ICESat-derived inland water surface spot heights (doi 10.1002/2015WR018237)





## RESEARCH ARTICLE

10.1002/2015WR017992

# Modeling grain size adjustments in the downstream reach following run-of-river development

Theodore K. Fuller<sup>1</sup>, Jeremy G. Venditti<sup>1</sup>, Peter A. Nelson<sup>2</sup>, and Wendy J. Palen<sup>3</sup>

<sup>1</sup>Department of Geography, Simon Fraser University, Burnaby, British Columbia, Canada, <sup>2</sup>Department of Civil and Environmental Engineering, Colorado State University, Fort Collins, Colorado, USA, <sup>3</sup>Earth to Ocean Research Group, Department of Biological Sciences, Simon Fraser University, Burnaby, British Columbia, Canada

### Key Points:

- The use of numerical models allows reasonable prediction of run-of-river (RoR) impacts
- Channels with high sediment supply conditions experience the greatest change in bed texture following development
- Channels with naturally high sediment supply recover quickly (~1 year) following a return of supply

### Correspondence to:

T. K. Fuller,  
tkfuller@sfu.ca

### Citation:

Fuller, T. K., J. G. Venditti, P. A. Nelson, and W. J. Palen (2016), Modeling grain size adjustments in the downstream reach following run-of-river development, *Water Resour. Res.*, 52, 2770–2788, doi:10.1002/2015WR017992.

Received 15 AUG 2015

Accepted 5 MAR 2016

Accepted article online 9 Mar 2016

Published online 9 APR 2016

**Abstract** Disruptions to sediment supply continuity caused by run-of-river (RoR) hydropower development have the potential to cause downstream changes in surface sediment grain size which can influence the productivity of salmon habitat. The most common approach to understanding the impacts of RoR hydropower is to study channel changes in the years following project development, but by then, any impacts are manifest and difficult to reverse. Here we use a more proactive approach, focused on predicting impacts in the project planning stage. We use a one-dimensional morphodynamic model to test the hypothesis that the greatest risk of geomorphic change and impact to salmon habitat from a temporary sediment supply disruption exists where predevelopment sediment supply is high and project design creates substantial sediment storage volume. We focus on the potential impacts in the reach downstream of a powerhouse for a range of development scenarios that are typical of projects developed in the Pacific Northwest and British Columbia. Results indicate that increases in the median bed surface size ( $D_{50}$ ) are minor if development occurs on low sediment supply streams ( $<1$  mm for supply rates  $1 \times 10^{-5} \text{ m}^2 \text{ s}^{-1}$  or lower), and substantial for development on high sediment supply streams (8–30 mm for supply rates between  $5.5 \times 10^{-4}$  and  $1 \times 10^{-3} \text{ m}^2 \text{ s}^{-1}$ ). However, high sediment supply streams recover rapidly to the predevelopment surface  $D_{50}$  (~1 year) if sediment supply can be reestablished.

## 1. Introduction

Renewable energy technologies are being promoted around the globe to mitigate the effects of climate change. River diversion, or run-of-river (RoR) hydropower, has emerged as a key renewable energy source [Jaccard *et al.*, 2011; Zhou *et al.*, 2009; Purohit, 2008; Dudhani *et al.*, 2006]. Small hydropower projects under ~100 MW primarily use RoR technology, whereas dams generating much larger amounts of energy rely on traditional storage-reservoir technology. Despite the relatively small physical footprint of RoR projects, there is growing concern that the development of multiple RoR projects within a watershed could degrade river and riparian ecosystems with physical and biological impacts similar in magnitude to those of large storage reservoir dams [Kibler and Tullis, 2013; Abbasi and Abbasi, 2011]. Concerns about salmonid species, in particular, are magnified due to the strong social, environmental, and cultural value placed on these fish species. Here we explore the potential for degradation of salmonid habitat downstream of RoR projects due to changes in bed material grain size caused by a sediment supply disruption. Surface grain size is a critical variable in the ability of salmonids to successfully spawn [Kondolf and Wolman, 1993; Riebe *et al.*, 2014], making it crucial to understand how RoR development will affect the range of grain sizes on the channel bed.

The impacts of large storage-based dams on river geomorphology are well documented. The most frequently observed geomorphic impact is storage of incoming bed load in the dam reservoir and incision downstream of the dam due to the loss of that sediment to the river [Williams and Wolman, 1984]. As the bed degrades, frequently under reduced discharges, fine sediment is preferentially winnowed from the bed, and the bed material coarsens [Harrison, 1950; Williams and Wolman, 1984; Wampler, 2004; Grant, 2012]. Channel morphology can also be impacted by a permanent storage of sediment by large dams because sediment supply is thought to be one of the primary controls on channel morphology and river channel bars [Church, 1992, 2006]. For example, Venditti *et al.* [2012] demonstrated experimentally that impoundment of sediment in a gravel-bedded stream can eliminate topographic and grain size heterogeneity

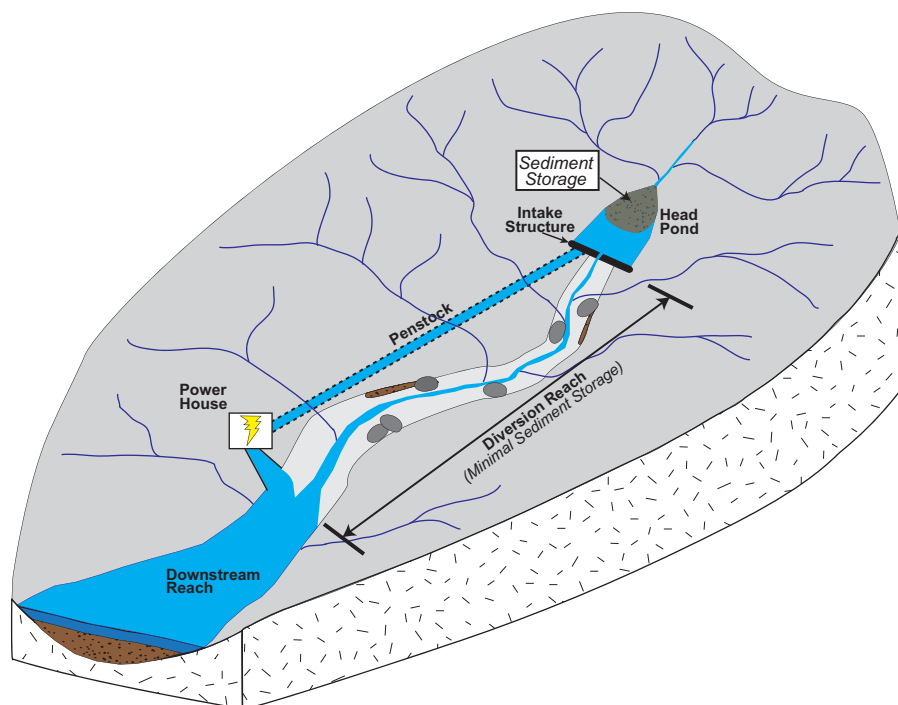


**Figure 1.** Schematic drawing of the major components of a typical RoR project in B.C., Canada, including the primary sediment storage element (i.e., the head-pond).

through lateral erosion of the river bars. It has also been shown that channel bars change their wavelength and amplitude due to changes in upstream sediment supply [Podolak and Wilcock, 2013]. Furthermore, reduction or elimination of peak flows following large dam closure has been documented to cause channel narrowing and simplification [Andrews, 1986; Allred and Schmidt, 1999; Merritt and Cooper, 2000; Grams and Schmidt, 2002], stranding bars and secondary channels [Allred and Schmidt, 1999; Grams and Schmidt, 2005], which are subsequently colonized by stabilizing vegetation [Graf, 1978; Knighton, 1988; Friedman et al., 1996a, 1996b; Grams and Schmidt, 2005]. The connection between higher habitat heterogeneity and higher species diversity has been supported at large biogeographic scales for a wide range of taxa and ecosystems [Kerr and Packer, 1997; Tews et al., 2004; MacArthur and MacArthur, 1961], including riverine fishes [Guégan et al., 1998]. As such, the coarsening of river beds and accompanying loss of topographic and grain size heterogeneity are widely thought to have deleterious effects on ecological communities and are common targets for river restoration efforts [Palmer et al., 2009].

The geomorphic impacts of RoR development are thought to be small relative to those of storage-based projects owing to their small size and design. Our examination of compliance documents for RoR projects in British Columbia indicates that they have relatively small head-ponds (typically  $<50,000 \text{ m}^3$ ), formed by dams that rise as much as 10 m above the local channel bed [Knight Piesold Ltd., 2008]. The head-pond serves to maintain a supply of water to the intake structure that diverts water into a penstock that bypasses the original river course (Figure 1). The diversion of water creates a reach of river with reduced flows during most of the year (the diversion reach, Figure 1). For steep-channel, high-head projects like those explored here, the diversion reach can be up to 5 km long and typically has a bedrock, boulder cascade, or step-pool morphology with little to no sediment storage. Diverted water is delivered to a powerhouse as much as 900 m below the head-pond where it is used to drive one or more turbines to generate electricity. After passing through the powerhouse, the diverted water is returned to the original channel such that flow in the reach downstream of the powerhouse (the downstream reach, Figure 1) is largely unaltered (with a possible exception during emergency facility shut-downs). RoR project designers take advantage of the steep channel gradients to maximize head. Consequently, diversion reaches of high-head RoR projects have channel slopes that range from 0.04 to 0.1 while downstream reaches typically have slopes  $< 10^{-2}$  [Knight Piesold Ltd., 2008; Cloudworks Energy Inc., 2011; Creek Power, 2012]. Modern RoR projects, like those explored

here, are equipped with adjustable weirs and/or sluice gates that are designed to pass flows in excess of the diversion capacity and evacuate trapped sediment from the head-pond. Although it varies between projects, diversion capacity is commonly 20% of the 2 year flood discharge. Thus, during dry years, the highest flows through the diversion reach will be significantly reduced, but during moderately wet years, the percentage of the total discharge diverted during a high flow event becomes less significant. At flows approaching the 10 year flood event, water intake is typically suspended to protect infrastructure [Ray, 2011]. During flood events, the head-pond weir can be lowered and the sluice gate opened to protect the intake structure and allow flood flows to pass through the diversion reach. As a result, the diversion reach could be subject to bed-load-transporting flows multiple times per year, similar in magnitude and frequency to the preproject bed-load-transporting flows. Annual exposure to these bed-load-transporting flows, combined with a lack of in-channel sediment storage [Kondolf and Matthews, 1991] and excess transport capacity that is typical of bedrock, boulder cascade, and step-pool channels [Montgomery and Buffington, 1997], makes it likely that the diversion reach rapidly transports bed load material evacuated from the head-pond downstream, beyond the powerhouse, and into the lower-gradient downstream reaches where the flow remains largely unaltered.

It is important to draw a distinction between “high-head” RoR projects, as described above, and “low-head” RoR projects. Low-head projects are typically located in moderate to low slope environments, are frequently designed without a diversion reach of any kind, and have a few to tens of meters of head [Anderson et al., 2014; Csiki and Rhoads, 2014; Skalak et al., 2009]. They can be found across the central and eastern regions of North America, though not exclusively. High-head projects, on the other hand, are located on steep channels, have tens to hundreds of meters of head, and require a concrete dam that rises several meters above the channel bed in order to create a head-pond of sufficient length and volume to supply water to the penstock. The result is a head-pond with depths at the downstream end that are several times greater than that of the channelized flood-flow depth entering the head-pond. This configuration creates areas of long-term dead storage within the head-pond despite efforts to evacuate sediment. Many projects have adjustable or deflating weirs that are lowered during high flow events (Figure 2a). Many other projects use fixed coanda screens for the intake and small sluice gates that are intended to pass sediment (Figure 2b). While some of the newest projects have large sluice gates capable of clearing a head-pond, most older projects do not. The result is a temporary sediment supply disruption to the diversion and downstream reaches, the duration of which depends primarily on the volume of dead storage within the head-pond. The diversion reach of high-head projects could also trap sediment on a long-term basis. However, the potential for long-term storage in the diversion reach is limited due to the typically steep, bedrock confined morphology [Knight Piesold Ltd., 2008]. In addition, the regular passage of bed-load-transporting flood flows through the diversion reach is sufficient to maintain the annual bed load transport capacity through the reach despite reduced flows during much of the year.

There have been a few investigations into the geomorphic impacts of low-head, non-energy-producing dams [Csiki and Rhoads, 2014; Skalak et al., 2009; Baker et al., 2011]. These studies have variously described bed coarsening, fining, or no geomorphic impact in the downstream reach. Others have reasoned that geomorphic impacts of modern RoR projects in general should be negligible owing to the ability of the projects to pass sediment [Kondolf, 1997; Kibler and Tullos, 2013]. To date, there has been no process-based, sediment-focused study of the geomorphic response of a river to a temporary sediment supply disruption caused by a high-head RoR project. The current approach to understanding the impacts of RoR development on sediment continuity is to monitor channel conditions following development. However, given the natural variability of sediment transport in steep mountain streams, the onset of a grain size impact may be difficult to detect. With so many projects recently completed or under construction around the world, the impacts of RoR development could be substantial before they are recognized.

Here we use a numerical model to explore the potential impacts of high-head RoR development on bed material grain size. Our focus is on the lower-gradient, downstream reach where the majority of high-value salmon habitat is located and where channel hydrology is largely unaltered. We explicitly ignore the diversion reach because it is not typically a sediment storage element in the system and because bed load transporting peak flows occur on a regular basis. In systems where this is not true, the diversion reach could represent a time-lag between dam closure and the disruption of supply to the downstream reach, an issue we address in our discussion. We begin by laying out a hypothesis for how RoR development may impact



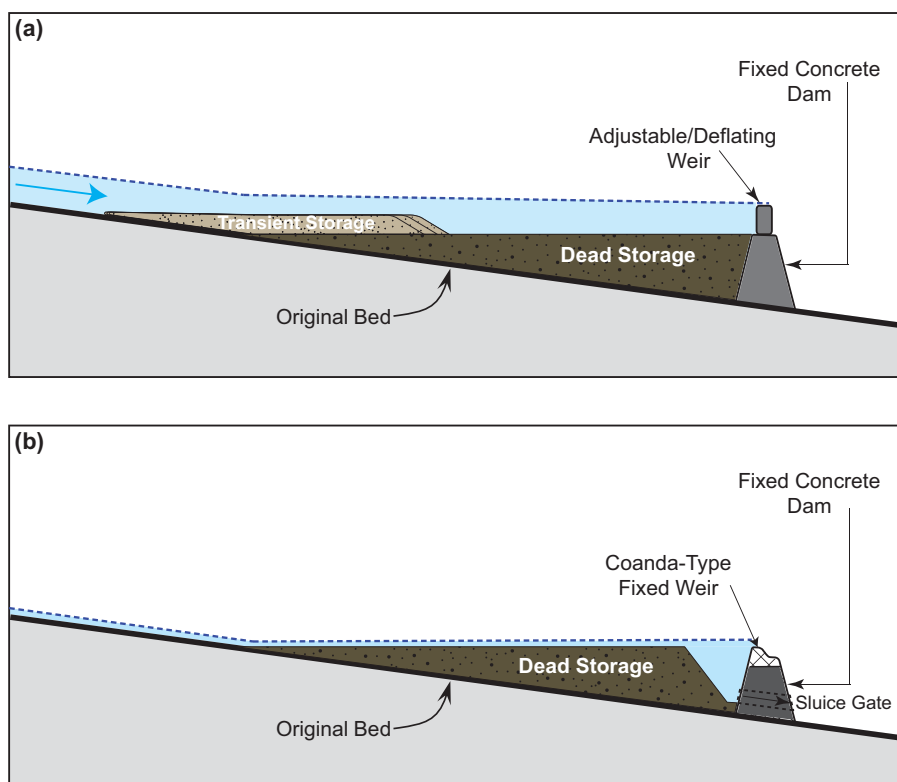


**Figure 2.** Schematic cross sections of typical head-pond configurations for high-head RoR projects that use: (a) adjustable or inflatable weirs and (b) fixed coanda-type weirs. Sediment is temporarily or permanently (i.e., dead storage) stored behind the fixed concrete dam that rises several meters above the channel bed. Figure adapted from Ray [2011].

bed sediment grain size in rivers due to temporary sediment supply reduction, followed by our specific research questions.

## 2. Hypothesized Bed Material Response to Sediment Supply Disruption

The rate at which bed load material is supplied to a gravel bed river exerts a strong control on the bed surface grain size [Kuhnle and Southard, 1988; Dietrich *et al.*, 1989; Buffington and Montgomery, 1999; Nelson *et al.*, 2009]. Channels adjust their slope and bed surface grain size so that the mean annual sediment load can be transported without aggradation or degradation [Parker and Klingeman, 1982; Parker and Toro-Escobar, 2002]. The sediment load and the subsurface material tend to have similar grain size distributions (GSD), while the bed surface is generally coarser than the subsurface [Parker and Klingeman, 1982; Whiting and King, 2003]. While this is not always true in upland gravel-bedded rivers [Lisle, 1995], it is typical. The armor ratio of the bed surface median grain size to that of the subsurface is dependent on sediment supply. In cases where bed load supply is well known, in laboratory experiments for example, it has been shown that channels with higher sediment supply per unit width have lower armor ratios than channels with low sediment supply per unit width [Dietrich *et al.*, 1989; Nelson *et al.*, 2009]. Experimental work has also shown that as sediment supply is reduced, the zone of active transport on the river bed narrows [Dietrich *et al.*, 1989; Lisle *et al.*, 1993; Nelson *et al.*, 2009; Venditti *et al.*, 2010], which serves to exacerbate bed coarsening because areas of the bed become coarse and inactive. In the field, it is more difficult to accurately determine bed load supply rates. However, among channels from similar geomorphic settings, those with a lower supply per unit width tend to be more strongly armored than channels with higher sediment supply per unit width [Lisle *et al.*, 2000].

Here we hypothesize that the sediment supply prior to RoR development exerts a strong control on whether, and for how long, there will be changes in the surface GSD downstream of high-head RoR projects. We expect significant changes in the surface GSD in channels with high sediment supply because

these channels are weakly armored. Restriction of sediment supply following RoR development will narrow the active transport corridor temporarily fining downstream bed load transport. Without upstream replacement of fine particles, the bed surface coarsens. Channels with low sediment supply are likely to be armored prior to development, so RoR development will have a lesser impact on the bed surface grain size. We further hypothesize that impacts of sediment supply reduction will be proportional to the dead storage volume in head-ponds of high-head projects (Figure 2).

We test these hypotheses using a 1-D morphodynamic model [Parker, 2004; Nelson *et al.*, 2009] to examine the response of channels immediately downstream of RoR projects to a temporary sediment supply disruption. We seek answers to the following questions: (1) what is the predicted magnitude of bed surface grain size change following RoR development?, (2) How does a channel's predam sediment supply regime affect its susceptibility to changes in grain size following development?, (3) Does RoR head-pond size influence the magnitude of the grain size impact?, and (4) What is the time scale of recovery for impacted channels following a reintroduction of sediment supply?

### 3. Methods

#### 3.1. Model Description

Here we use a 1-D morphodynamic model, developed by Parker [2004] and implemented by Nelson *et al.* [2009], to predict the response of the downstream reach (Figure 1) to a disruption in sediment supply. The model and its variants [Parker, 1990, 1991; Cui *et al.*, 1996, 2003, 2006a, 2008; Nelson *et al.*, 2009; Viparelli *et al.*, 2010] have provided reasonable approximations of the morphodynamic change in plane bed and bar-pool gravel-bedded systems and should be well suited to predicting potential morphodynamic change in the downstream reach in response to changes in sediment supply. The main input parameters to the model include the initial GSD of the subsurface, the initial slope, the sediment supply rate, water discharge, and channel width. The GSD of the bed load supply is assumed to be that of the subsurface and the GSD of the surface is allowed to evolve from the subsurface GSD prior to a sediment disruption event (see section 3.2 below). The modeled reach is spatially discretized into computational nodes. At each node, the model calculates shear stress using the normal flow approximation. The transport of bed load is calculated using the surface-based relation of Parker [1990] in the case of gravel bed load or the relation of Wilcock and Crowe [2003] in the case of a sand-gravel mixture. The model calculates changes in bed surface elevation and grain size using the 1-D mixed-grain size Exner equation with the active layer assumption [Parker, 2008].

#### 3.2. RoR Model Scenarios

We modeled hypothetical sediment disturbance scenarios based on three field sites that are representative of watersheds in the U.S. Pacific Northwest and British Columbia. We refer to the sites as "cobble," "coarse gravel," and "gravel" based on their respective grain size distributions (Figure 3). All three watersheds are located in the southern Coast Mountains of the Canadian Cordillera in British Columbia and all three have RoR projects that have been approved for construction or recently constructed. The modeled watersheds range in size from approximately 80–130 km<sup>2</sup> with a history of glaciation and reworked fluvial sediments in the valleys. In general, the modeled watersheds experience peak flows in late spring and early summer due to snowmelt events and then again in late fall due to rain events. The smallest watershed of the three (the gravel site) has the highest mean elevation and had a larger portion of its total watershed area occupied by glaciers in the past. The hydrology of this watershed is more strongly influenced by the spring snowmelt than the other two watersheds with less pronounced peak flows in late fall.

In each watershed, the upper reach of the main-stem channel is characterized by a bedrock, boulder cascade, or step-pool morphology. This is the reach that has or will become the diversion reach. The lower reach, downstream of the proposed powerhouse location, is characterized by an alluvial plane bed or bar-pool morphology. This pattern of channel morphology along the different sections of a RoR project is nearly universal among RoR projects in B.C. and is driven by the desire to maximize the head between the intake structure and the powerhouse in order to maximize the energy capacity of the project. We only model the reach downstream of the proposed powerhouse, where the profile concavity is negligible.

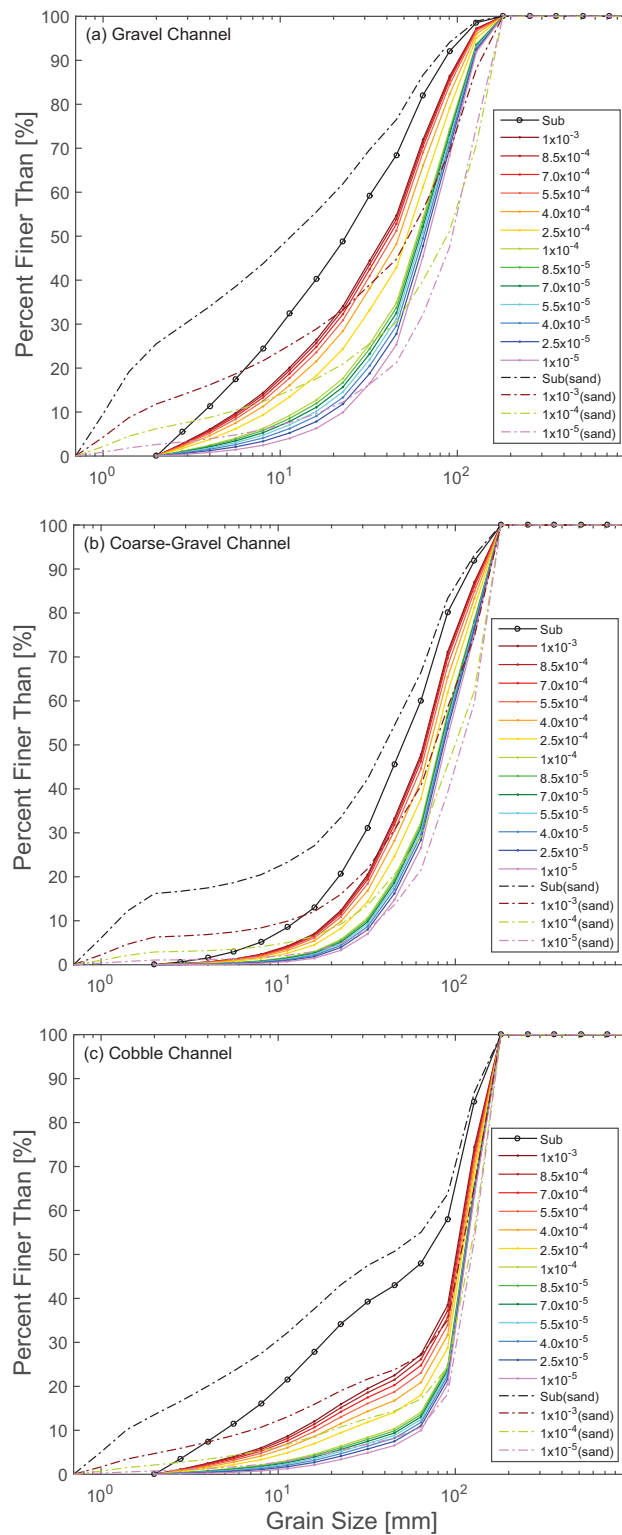


**Figure 3.** Subsurface (black circle) and equilibrium surface grain size distributions (solid colored lines) are shown for each of the three channel types discussed in the text: (a) gravel, (b) coarse-gravel, and (c) cobble. The legend indicates the preproject sediment supply rate in  $\text{m}^2 \text{ s}^{-1}$  for each equilibrium distribution (the equilibrium distributions for the two lowest model supply rates ( $5 \times 10^{-6}$  and  $7.5 \times 10^{-6}$ ) are not substantially different from that of  $1 \times 10^{-5}$  and thus are not shown). Also shown are distributions using the sand-gravel GSD and the Wilcock and Crowe [2003] bed load relation (dashed lines).

At each field site, we measured the GSD of the surface and subsurface bed material, the water-surface slope, and bankfull channel dimensions (Table 1). Discharge data available from the Water Survey of Canada or RoR project developers were used to estimate typical bankfull discharges. A surface GSD was obtained by spray painting a  $1 \times 1 \text{ m}^2$  of an exposed bar surface and measuring the size distribution of all painted particles. We also measured the surface size distribution using line-by-number Wolman counts. We measured the subsurface GSD using a volumetric sampling technique in which surface material is first removed from the  $1 \times 1 \text{ m}^2$  grid to a depth matching the base of the largest surface particle [Bunte and Abt, 2001]. Subsurface sediment is then collected from within the square meter to a depth equal to the surface  $D_{90}$  such that the volume of subsurface material collected is roughly  $1 \text{ m}^2 \times D_{90}$  (typically a depth of 0.35–0.45 m). The subsurface GSD measured in the field was used as the initial GSD of the subsurface, bed surface, and the sediment load in the model. We did not use the measured surface size distributions for our model because it is not clear what flow and sediment supply conditions the surface reflected at the time of measurement.

We undertook two sets of simulations to explore changes along a 1 km section of channel. We are mainly interested in how RoR development impacts the behavior of coarse bed material in these watersheds because of the important role that gravel size plays in salmonid habitat. Sand moves through these systems as suspended load at low flows and as washload at channel forming bankfull flows.

**Table 1.** Input Parameters for Morphodynamic Model as Measured in the Field

Variables	Units	Channel Types		
		Cobble	Large-Gravel	Gravel
Water discharge <sup>a</sup>	m <sup>3</sup> s <sup>-1</sup>	35.8	30.2	34.7
Initial bed slope	[1]	0.0081	0.0086	0.0076
Bankfull width	m	20.1	20.4	22.5
Initial subsurface $D_{50}$ <sup>b</sup>	mm	69	50	23
Initial subsurface $D_{90}$ <sup>b</sup>	mm	144	121	84

<sup>a</sup>Bankfull discharge estimated from Water Survey of Canada historical data or from data provided by RoR operators.

<sup>b</sup>Grain size values are for the distributions truncated at 2 mm.

Therefore, our primary set of simulations use the *Parker* [1990] surface-based bed load transport relation and GSDs truncated at 2 mm. However, transient sand cover on the bed surface could impact our results, so we undertook a secondary subset of simulations using the *Wilcock and Crowe* [2003] relation with the GSD truncated at 0.7 mm.

Prior to each simulation, the bed surface was allowed to equilibrate to the

imposed conditions by conducting zeroing runs [e.g., *Cui et al.*, 2006a, 2006b; 2008]. Cumulative grain size distributions of the input GSD and the equilibrated bed surfaces are shown in Figure 3. The duration of the zeroing runs was set to 250 days of bankfull flow for all model scenarios, with the exception of two runs that used a 15 km domain (see below). We found that all 1 km model runs reached a steady state (no substantial change in topography or grain size) within this time period, even at the lowest sediment supply rates, which take the longest to reach steady state.

The model assumes a simplified hydrograph of either geomorphically *effective* or *ineffective* flows and incorporates an intermittency factor to account for the annual duration of geomorphically effective flow [*Parker*, 2004]. We use an intermittency factor of 0.014 corresponding to an effective flow duration of 5 days of bankfull flow per year, roughly the midrange of effective flow duration reported in the literature [*Andrews*, 1980; *Lenzi et al.*, 2006; *Endreny*, 2007; *Hassan et al.*, 2014].

Model scenarios presented here are limited to a single sediment disruption event in which all bed load supplied to the downstream reach is stopped for a period of time before being restored. This type of disruption scenario is consistent with the infilling of dead storage volume following initial closure of the dam. Field observations of long-term sediment storage in the head-pond of our gravel site suggest sediment storage capacity on the order of  $5 \times 10^3 \text{ m}^3$ , which can be a substantial disruption of sediment supply to the downstream reach. The choice to model a single, but temporary, sediment disruption event linked to the infilling of dead storage is also supported by compliance documents that indicate that the vast majority of new projects in southwestern B.C. are designed with adjustable weirs that sit on top of fixed concrete dams that rise several meters above the channel bed [*Knight Piesold Ltd.*, 2008; *Cloudworks Energy Inc.*, 2011; *Ray*, 2011; *Creek Power*, 2012]. On steep channels, this design creates head-ponds that deepen downstream and are substantially deeper than flood-flow depth at the base of the dam. With this configuration, sediment cannot be efficiently passed over the weir until the base of the head-pond aggrades to the top of the fixed concrete dam. While sluice gates may allow for the evacuation of sediment located directly behind the gate during this period of head-pond aggradation, sediment supply to the diversion and downstream reaches should be substantially reduced until the volume of dead storage has been filled. We do not explicitly treat sediment transport in the diversion reach given the complexity in accurately modeling bed load transport in steep channels [e.g., *Yager et al.*, 2007], the fact that bed load capacity greatly exceeds the supply in these reaches and the observation that there is little storage space within these reaches. Instead we assume the diversion reach serves only to provide a yet unknown lag between dam closure upstream and sediment disruption downstream, without any effect on the caliber or quantity of sediment being transported through the system.

We ran 120 model scenarios for each site using the *Parker* [1990] bed load relation; 15 preproject sediment supply rates for eight different supply disruption time scales ( $T_s$ ). To keep model run times tractable, a 1 km reach with 50 computational nodes was used. The model reach is assumed to be immediately downstream of the powerhouse where all water has been returned to the channel. To help constrain maximum and minimum input values for the preproject bed load supply rates, we refer to a study conducted in the coastal mountains of B.C. that analyzed a delta deposit in an alpine lake to generate a 52 year record of sediment flux [*Pelpola and Hickin*, 2004]. The channel analyzed in that study has since been developed into a RoR project and thus provides an estimate of typical bed load supply rates for channels that are candidates for RoR development. We take the bed load flux per square kilometer of watershed area estimated by *Pelpola and*

Hickin [2004] ( $\sim 1 \times 10^{-5} \text{ m}^2 \text{ s}^{-1}$ ) and multiply it by the watershed area of the RoR field sites modeled here to get a representative bed load supply rate per unit width for each site. We varied the bed load supply rate in the model by half an order of magnitude below and 2 orders of magnitude above this value, resulting in a range of  $5 \times 10^{-6} - 1 \times 10^{-3} \text{ m}^2 \text{ s}^{-1}$  (see Figure 3 for the specific bed load supply rates used). Reducing bed load supply below  $5 \times 10^{-6} \text{ m}^2 \text{ s}^{-1}$  produced conditions that did not respond to sediment supply reduction.

The time scale of sediment disruption was varied by a factor of 60 across eight different  $T_s$  values (0.2, 1, 2, 3, 4, 6, 8, and 12 years). Based on a midrange supply rate of  $2.5 \times 10^{-4} \text{ m}^2 \text{ s}^{-1}$  and head-pond volumes ranging from 50,000 to 2500  $\text{m}^3$ , the time required to fill the dead storage volume with sediment (assumed to be half the total head-pond volume) ranges from 11 years down to 1 year, respectively. At lower supply rates,  $T_s$  can be considerably longer. Keeping all other variables constant, the channel is allowed to evolve for the prescribed  $T_s$ . Following the period of sediment disruption, the predevelopment bed load supply is returned to the downstream reach and the channel is allowed to readjust to the imposed sediment load.

To explore the potential for downstream attenuation of impacts, we ran two supplementary simulations with a 15 km model reach comprised of 1500 nodes with an extended equilibrium period (10,000 days at bankfull flow). These supplementary simulations had conditions that match those of the gravel site with a moderately high sediment supply rate of  $5.5 \times 10^{-4} \text{ m}^2 \text{ s}^{-1}$  and sediment disruption time scales of 1 and 8 years. Just like the primary set of model runs, the supplementary runs consist of a single disruption to sediment supply during which the reach is completely starved of sediment.

### 3.3. Model Specifications

In our application, we initialize the model with a linear long profile, which is reasonable over the short ( $\sim 1$  km) reach lengths we explore downstream of the powerhouse. A concave profile with a backwater approximation [cf. Hoey and Ferguson, 1994; Ferguson and Church, 2009; Ferguson et al., 2015] may be more appropriate over much longer reach lengths, but that would substantially complicate our initialization or “zeroing” runs. Fortunately, weak profile concavity in the model should have little impact on the model results. Model calculations are performed at each computational node (50 nodes, each 20 m in length) on a unit-width basis using a fixed channel width (Table 1) along the entire modeled reach with a uniform, rectangular cross section. Cui et al. [2008] has shown that channels with complex topography can be simulated using a 1-D model, providing that the model is width averaged over individual topographic units. Our use of a uniform cross section is in recognition of this earlier work.

The normal flow model used here is consistent with the version available online in Parker [2004], which provides users with the ability to implement the model without modification. Parker [2004] uses the Manning-Strickler resistance formulation to estimate flow depth with a roughness height of  $2D_{90}$  (90th percentile of the bed surface grain size distribution). Total shear stress on the bed is calculated as the depth-slope product. Recent work suggests that the Manning-Strickler relation systematically underestimates flow resistance in channels with low relative submergence ( $d/D_{84}$ ) [Ferguson, 2007; Rickenmann and Recking, 2011], where  $d$  is flow depth and  $D_{84}$  is the 84th percentile of the bed surface grain size distribution. Our flows consistently meet or exceed the threshold where problems are thought to occur:  $d/D_{84} < 4$  [Ferguson, 2007] and  $d/D_{84} < 7$  [Rickenmann and Recking, 2011].

The Parker [2004] model includes a parameterization of the active layer thickness ( $L_a$ ) as well as a sediment mixing parameter ( $\alpha$ ) [Hoey and Ferguson, 1994] that determines the composition of sediment exchanged between the surface and subsurface during aggradation or degradation. The value of  $L_a$  has the potential to limit degradation depth during a single time step, thereby affecting the adjustment time scales. During aggradation, the elevation of the boundary between the active layer and the subsurface increases, resulting in an exchange of sediment into the subsurface layer. The parameter  $\alpha$  specifies the fraction of this exchange material that is made up of active layer sediment, and  $(1 - \alpha)$  specifies the fraction made up of bed load material. Because the grain size distributions of the active layer sediment and the bed load material can be quite different, the choice of  $\alpha$  can potentially affect the amount of time required for the surface grain size distribution to recover to preproject conditions following the reestablishment of sediment supply.



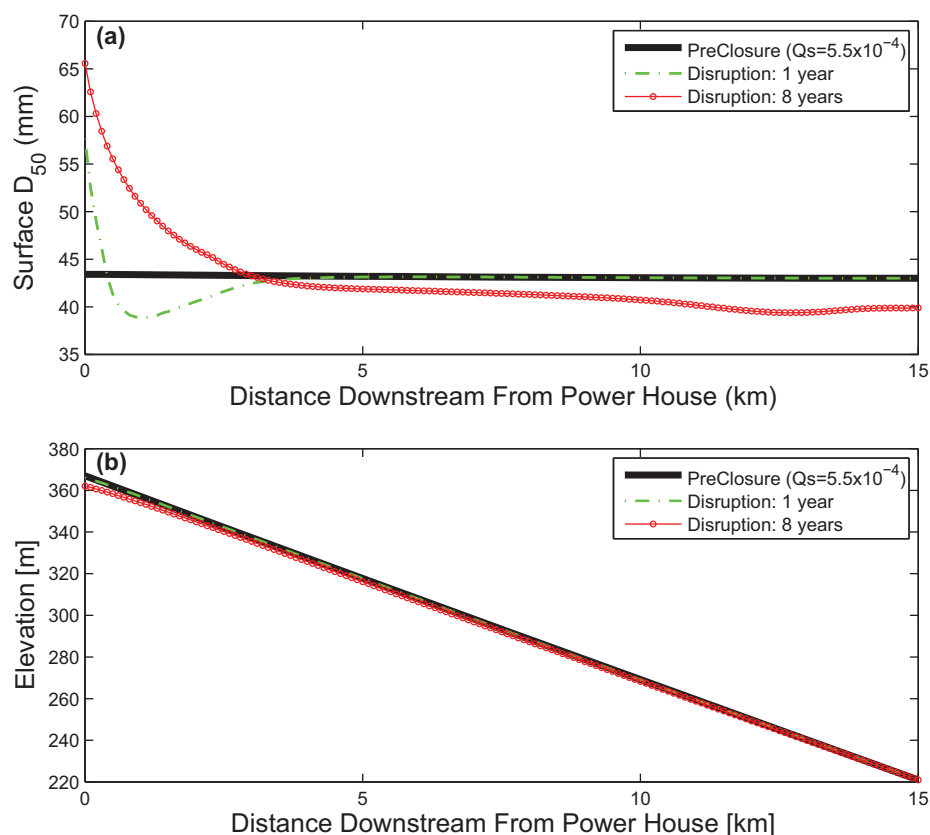


**Figure 4.** Longitudinal profiles of the (a) median surface grain size and (b) bed elevation for the 15 km model run with conditions that match those of the gravel bed channel and a moderately high sediment supply rate of  $5.5 \times 10^{-4} \text{ m}^2 \text{ s}^{-1}$ . Profiles shown include the predisruption equilibrium profile (black), the profile following a 1 year disruption period (dashed green), and the profile following an 8 year sediment disruption period (red circles).

We set  $L_a$  equal to bed surface  $D_{90}$ . Increasing  $L_a$  has no effect on our results because the bed does not erode to a depth  $> D_{90}$  in any single time step. We confirmed this by conducting nine “sensitivity” model runs (three for each channel type using low, moderate, and high sediment supply rates) using a value of  $2D_{90}$  for  $L_a$ . Results from these sensitivity runs show the same change in bed elevation as that predicted in the primary set of model runs where  $L_a$  is equal to  $D_{90}$ .

Previous applications of this morphodynamic model have set  $\alpha$  to values ranging from 0.7 for investigation of sediment pulses in mountain rivers [Cui and Parker, 2005; Cui et al., 2003] to 0.2 for an investigation of gravel augmentation practices [Viparelli et al., 2011] and to 0.5 for an investigation of the effects of a cycled hydrograph on surface grain size [Parker et al., 2007]. We chose  $\alpha = 0.5$  for our application so that the model incorporates equal amounts of surface and bed load material into the aggrading deposit. Sensitivity analysis using  $\alpha$  values of 0.2 and 0.8 revealed that its value has negligible effect on the magnitude of grain size change, but it does impact the recovery time once sediment supply is restored. We discuss these results below.

#### 4. Results

We modeled the change in surface grain size downstream of the powerhouse following a single sediment disruption event associated with RoR development. Results from the supplementary 15 km model runs show strong attenuation of the geomorphic impacts with distance downstream from the powerhouse (Figure 4). The longitudinal profile of the surface  $D_{50}$  shows coarsening is strongly attenuated within the first 0.5 km downstream of the powerhouse for the 1 year disruption time scale and the first 3 km for the 8 year disruption time scale (Figure 4a). Bed elevation change is minimal for the 1 year disruption time scale (0.75 m immediately downstream of the dam and  $< 0.5$  m downstream of 0.2 km; Figure 4b). Bed elevation

change is more substantial for the 8 year disruption time scale with bed degradation of  $\sim 5$  m immediately downstream of the dam and tapering to a 1 m decrease in elevation that persists for  $\sim 9$  km downstream of the powerhouse (Figure 4b). For both the long and short disruption times scales, there is a moderate ( $\sim 5$  mm) bed fining downstream of 3 and 0.5 km, respectively (Figure 4a), caused by delivery of fine sediment stripped from upstream reaches. The 1 year supply disruption simulation completely recovered from the fining by 5 km from the powerhouse. Grain size fining in the 8 year supply disruption persists through the entire model domain because the material is stable at the new lower gradient. The attenuation of impacts with distance downstream indicates that the greatest changes in both grain size and bed elevation occur within the first km downstream of the powerhouse. We therefore focus our simulations on the reach immediately downstream of the powerhouse, where impacts are likely to be most severe in response to a temporary sediment supply disruption caused by RoR development.

Using the change in median grain size near the dam as an index of geomorphic impact, our 1 km model results indicate that preproject sediment supply rate exerts the strongest control on the magnitude of grain size change in response to a sediment supply disruption. Changes in the surface  $D_{50}$  through time (Figure 5) reveal that the largest change occurs in the scenarios with the highest preproject sediment supply rates. In the gravel channel (Figure 5a), for example, the highest preproject sediment supply scenario shows an increase in the surface  $D_{50}$  from 38.5 to 67 mm in response to dam closure (a 74% increase). In contrast, the lowest preproject sediment supply scenario shows an increase in the surface  $D_{50}$  from 68.5 to 69.5 mm (a 1% increase). Similar patterns can be observed for the coarse gravel and cobble channels (Figures 5b and 5c), but the magnitude of the grain size change decreases with increasing bed material size.

The time scale of disruption, dictated by the time it takes to fill the dead storage within the head-pond, exerts a secondary control on the magnitude of the bed surface response. The effect of  $T_s$  can be seen by comparing the long and short supply disruptions in Figure 5. For the coarse gravel site (Figure 5b), the high preproject sediment supply scenario predicts that the surface  $D_{50}$  will increase from 66 to 81 mm during the 1 year  $T_s$  compared to a maximum  $D_{50}$  of 86 mm at the end of the 8 year  $T_s$ , where the time in years assumes 5 days of bed load transporting flows per year. This comparison between short and long supply disruptions shows that the majority of the increase in the  $D_{50}$  occurs rapidly following dam closure (75% of the maximum increase in the  $D_{50}$  is predicted to occur within the first 12.5% of the total disruption time). This effect is less pronounced in the midrange (blue line) and low (green line) preproject sediment supply scenarios (Figures 5a–5c).

Tracking the change in the surface  $D_{50}$  through time also sheds light on the time it takes for the channel to return to its preproject bed surface condition once sediment supply is reestablished. The “recovery time” of the channel, defined here as the time required for the surface  $D_{50}$  to stabilize within 1% of preclosure values (i.e., equilibrium value) following the return of sediment supply, appears to be inversely related to the rate of preproject sediment supply (Figure 5). In the highest sediment supply scenarios, the recovery time is roughly a year regardless of the bed material type (assuming 5 days of bankfull flow conditions per year). In contrast, the recovery time for scenarios with midrange sediment supply rates ranges from 2 to 4 years. Low preproject supply scenarios do not completely recover to preproject  $D_{50}$  values during the time of simulation, although all low-supply scenarios in the primary set of model runs recover to within less than 1 mm of the preproject values.

The results of our sensitivity analysis indicate that recovery time is sensitive to the value assigned to  $\alpha$  in the model. For a gravel bed channel with a moderate sediment supply rate ( $1 \times 10^{-4}$ ) and  $T_s = 8$  years, a value of  $\alpha = 0.2$  (more bed load material in the exchange fraction) results in a recovery time of 8 days of bankfull flow conditions (1.6 years). With  $\alpha = 0.5$ , the value we used in our simulations, recovery took 20 days, at bankfull flow conditions (Figure 7). With  $\alpha = 0.8$  (less bed load material in the exchange fraction), recovery took 49 days of bankfull flow conditions (9.8 years). We see no reason to expect that the fractional component of bed load material incorporated into the aggrading deposit would deviate substantially from 0.5, however, the sensitivity of our results to the value of  $\alpha$  should be considered in application of our modeling procedure.

Results from the secondary set of model simulations using a GSD truncated at 0.7 mm and the gravel-sand transport relation of *Wilcock and Crowe* [2003] show that inclusion of the sand fraction increases the simulated grain size change by a factor of 1.3–1.6 compared to the change predicted using the sand-free GSD

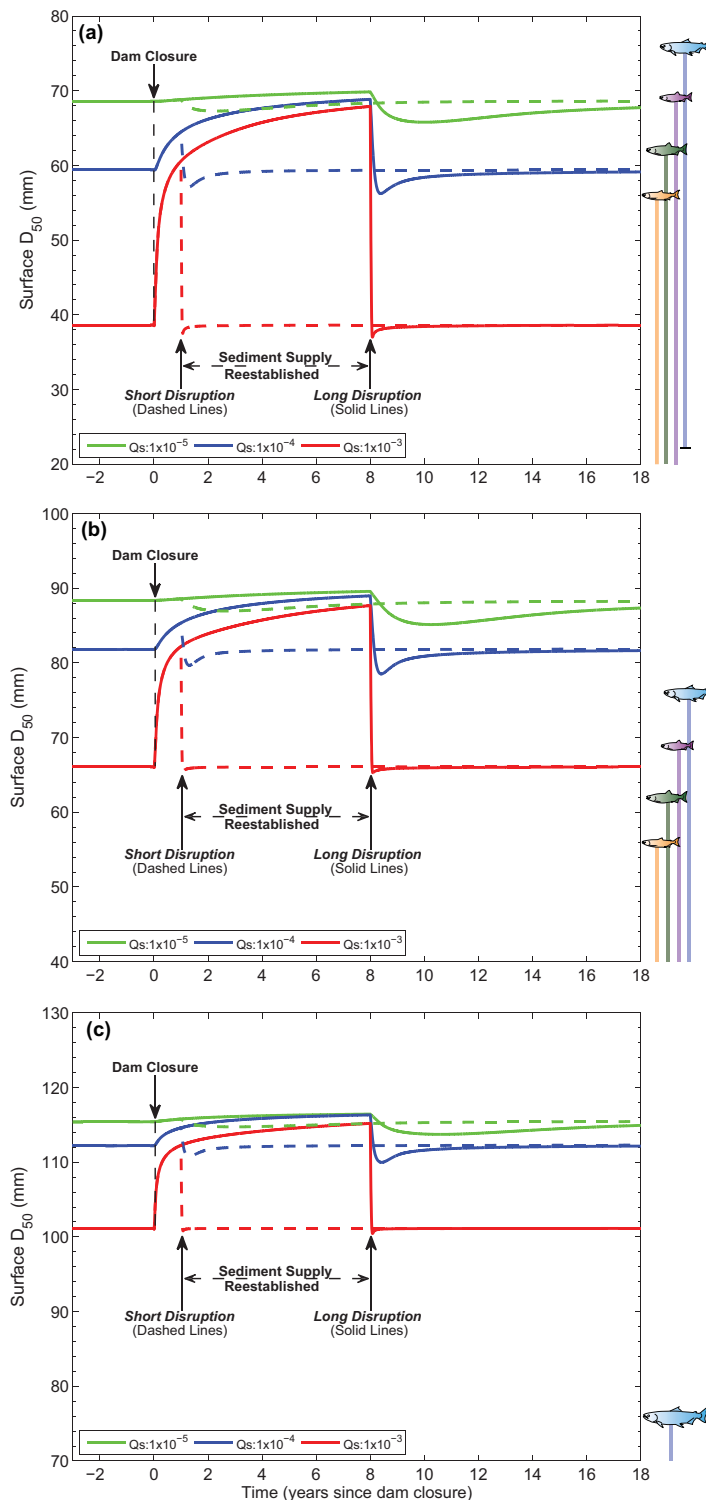


**Figure 5.** Change in surface  $D_{50}$  through time for different sediment supply rates and disruption time scales in (a) gravel, (b) coarse-gravel, and (c) cobble-bedded channels. Three sediment supply rates are shown for each channel ( $1 \times 10^{-3} \text{ m}^2 \text{ s}^{-1}$  (red);  $1 \times 10^{-4} \text{ m}^2 \text{ s}^{-1}$  (blue);  $1 \times 10^{-5} \text{ m}^2 \text{ s}^{-1}$  (green)). Solid lines track the surface  $D_{50}$  through time for a long disruption scenario (8 year disruption time scale). Dashed lines track the surface  $D_{50}$  for a short disruption scenario (1 year disruption time scale). Time along the x axis assumes 5 days of bed load transporting flows per year. Data are from the sand-free model runs. Fish icons and vertical bars show the range of suitable spawning grain size for Chinook (blue, 22–76 mm), Pink (purple, 8–69 mm), Chum (green, 14–62 mm), and Sockeye (orange, 15–56 mm) salmon. The upper end of spawning ranges reflects a weighted average of data from Riebe et al. [2014] while the lower end reflects the 25th percentile of data from Kondolf and Wolman [1993]. Riebe et al. [2014] do not report data for Chum salmon so we use the coarsest observation from Kondolf and Wolman [1993] as the upper end of the Chum salmon range. The lower end of the spawning ranges noted above fall below the scale of the plots in many cases.

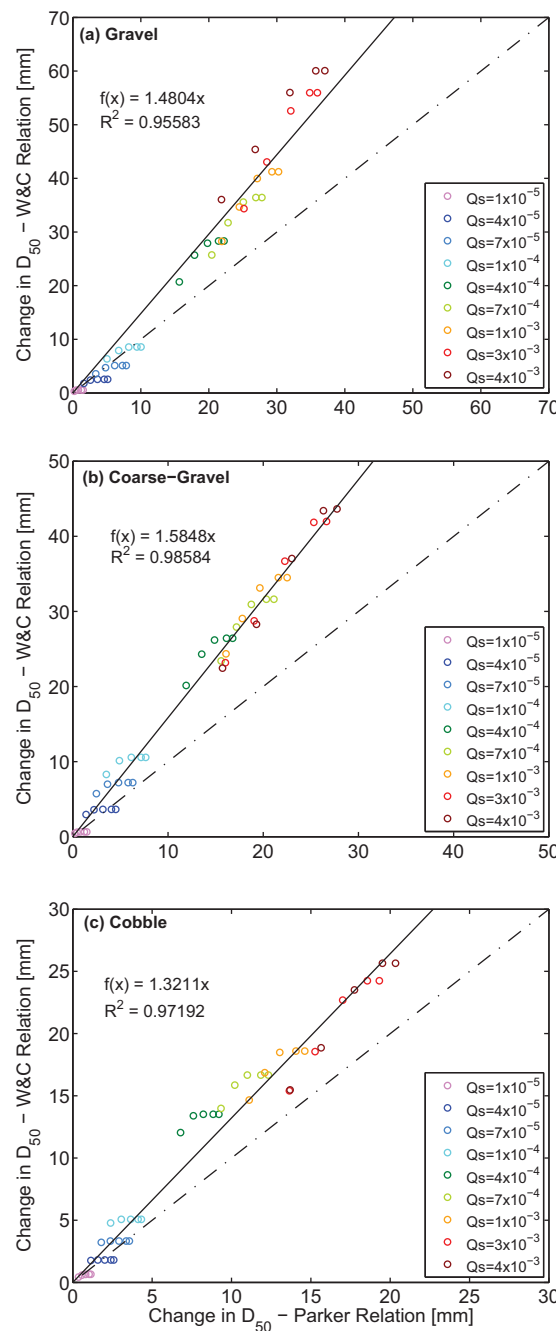


**Figure 6.** The maximum change in the surface  $D_{50}$  predicted by the gravel-sand relation [Wilcock and Crowe, 2003] relative to that predicted by the sand-free relation [Parker, 1990] for the three channel types: (a) Gravel, (b) Coarse Gravel, and (c) Cobble. Solid line and equations show the least squares linear fit to the data. Dashed line shows a 1:1 relation. Data points are colored according to the preproject sediment supply. Each supply rate has five data points, one for each value of  $T_s$  (see text).

supply and  $T_s$  using the Parker [1990] simulations. The morphodynamic model predicts substantial change in the surface  $D_{50}$  will occur when the preproject sediment supply is high and the time scale of disruption exceeds a few years. As indicated by the shallow sloping contour lines at the bottom of each plot in Figure 8, small adjustments in disruption time will have a greater impact than the initial bed load supply rate for short disruption time scales. This suggests that grain size change is most sensitive to head-pond size when the

and the Parker [1990] bed load transport relation (Figure 6). The secondary set of simulations (45 secondary simulations for each channel type: 9 sediment supply rates and 5 disruption time scales) predict longer recovery times compared to the sand-free set of simulations. In general, it takes twice as long to reach the stable asymptote shown in Figure 5 following the return of sediment supply in the secondary set of simulations (Figure 7). It is difficult to assess whether these results reflect differences in the transport model behavior or differences in sediment behavior in the system. The Parker [1990] relation (used in the primary set of simulations) includes a hiding function that causes the ratio of a size fraction in the load relative to that in the bed surface to decline monotonically with grain size. This means that finer material is preferentially transported, with respect to its presence on the bed surface. The Wilcock and Crowe [2003] relation (used in the secondary set of simulations) has a similar hiding function, but size selective transport can occur. In effect, sand reduces the threshold of motion for the fine and moderately sized materials while the coarser sizes remain weakly mobile or immobile in the model. This has the effect of making the zeroing run  $D_{50}$  coarser in the Wilcock and Crowe [2003] simulations than in the Parker [1990] simulations because the moderately sized material is depleted from the reach. The differences between the primary and secondary set of model runs described above are limited to the magnitude of predicted change, equilibrium surface grain size, or time required to recover equilibrium conditions. Qualitatively, however, the two sets of model runs behave similarly in their response to the two primary variables explored in this study (see discussion of Figure 8 below). Given our observation that there is little sand on the bed surface, even at low flows, we regard the Parker [1990] simulations as more closely matching the prototype channels. Nevertheless, it is clear that the presence of sand on the surface can affect our results and needs to be considered when there is persistent sand coverage at high flows.

Figure 8 shows the maximum change in the surface  $D_{50}$  as a function of preproject sediment

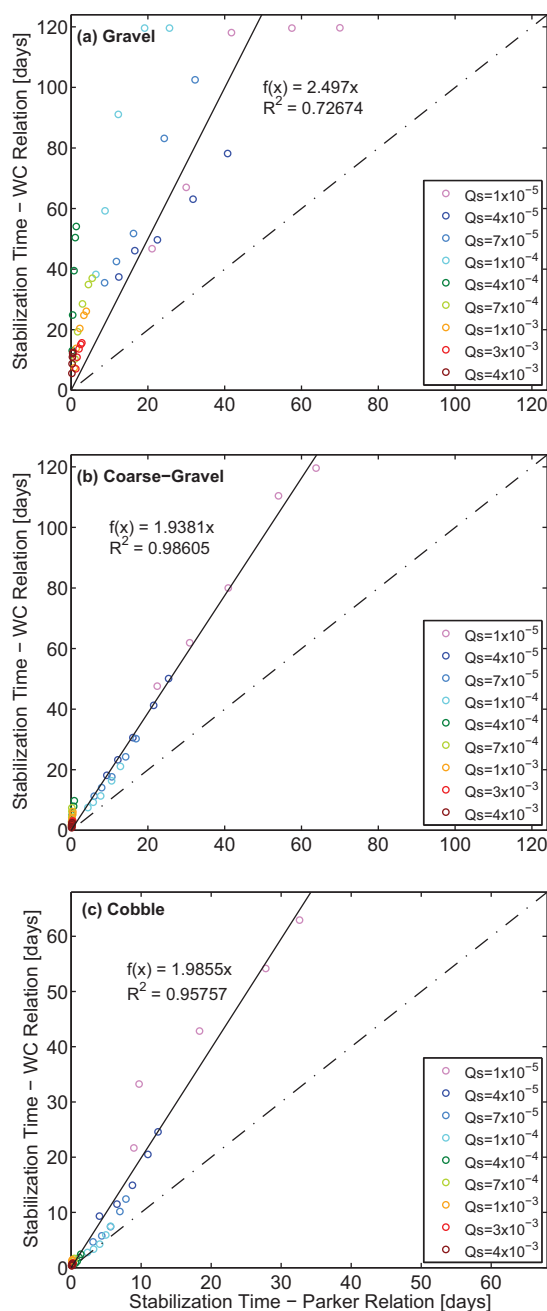


**Figure 7.** Time required for the surface  $D_{50}$  to stabilize at preproject values following a return of sediment supply as predicted by the gravel-sand relation [Wilcock and Crowe, 2003] and the sand-free relation [Parker, 1990]. Plots are for the three channel types: (a) Gravel, (b) Coarse Gravel, and (c) Cobble. Symbols are the same as in Figure 6.

sediment supply disruption. At these higher supply rates, the magnitude of change in the surface  $D_{50}$  depends on both the specific supply rate and the time scale of disruption.

Our results suggest that there is a class of channels with high sediment supply that could be substantially impacted by RoR development. An increase in the surface  $D_{50}$  of as much as  $\sim 30$  mm or roughly 74% of the predevelopment  $D_{50}$  is possible in these channels. In the case of high sediment supply, the magnitude of change in the surface  $D_{50}$  is sensitive to increasing head-pond size up to a point where the head-pond is capable of capturing at least a full year of bed load material. Further increases in head-pond size have

head-ponds are small ( $\sim 2500$  m<sup>3</sup>) to moderately sized ( $\sim 5000$  to  $10,000$  m<sup>3</sup>). For head-ponds larger than moderate size, changing the head-pond size of a project has minimal impact on the maximum change in the surface  $D_{50}$  (as indicated by the nearly vertical contour lines in the upper two-thirds of the plots in Figure 8). This indicates that bed load supply is the more important factor for longer time scales of disruptions and, by proxy, projects with larger head-ponds. Comparison of Figures 8a–8c highlights the differences in the magnitude of the bed surface response between the three sites in the primary set of model runs. The maximum change in the surface  $D_{50}$  is greatest in the gravel channel (30 mm increase; Figure 8a) and least in the cobble channel (14 mm; Figure 8c). Identical plots using results from the secondary set of model runs exhibited the same characteristics described above and differed only in the contour line values. For simplicity, we do not include those plots here.

## 5. Discussion

The modeling reveals that channels with low sediment supply are not at risk of substantial bed surface coarsening as a result of project development because the channels are already adjusted to having low sediment supply. In fact, we predict that changes in bed surface grain size in low sediment supply channels are so small ( $\sim 1$  mm increase in surface  $D_{50}$ ) they would be difficult to detect in the field. If we accept a supply rate of  $1 \times 10^{-5}$  m<sup>2</sup> s<sup>-1</sup> as typical for mountain environments in the Pacific Northwest and B.C. based on the work of Pelipola and Hickin [2004], the geomorphic impacts of RoR development on these channels will be minimal. In this case, the size of the head-pond (i.e., disruption time scale) plays a very limited role in determining the magnitude of change in the surface  $D_{50}$  (Figure 8). As the predevelopment sediment supply rate increases to 1 and 2 orders of magnitude greater than this “typical” supply rate, the surface  $D_{50}$  becomes more sensitive to the



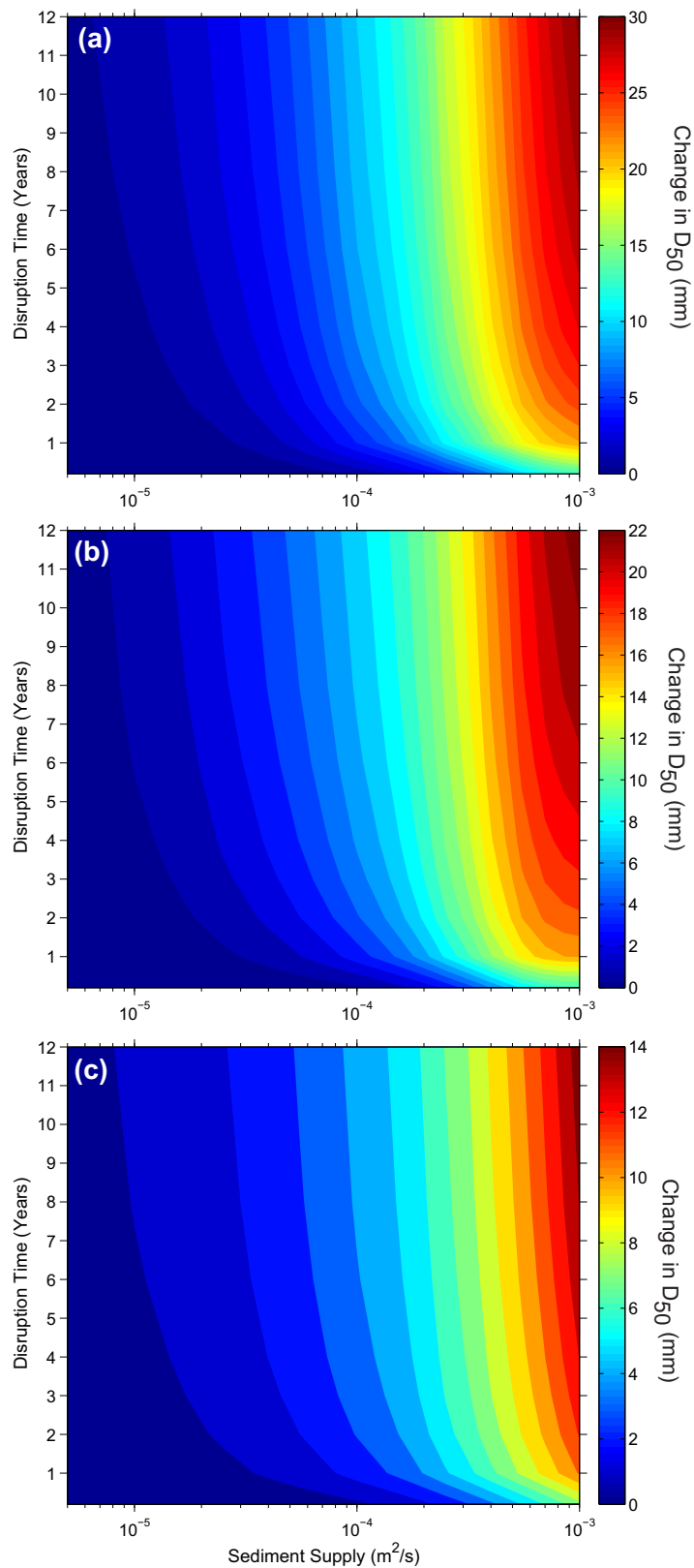


**Figure 8.** Maximum change in the surface median grain size ( $D_{50}$ ) as a function of preproject sediment supply and disruption time scale for (a) gravel, (b) large-gravel, and (c) cobble-bedded channels. Maximum change is calculated from the time of dam closure to the time sediment supply is reestablished.

decreasing influence on the magnitude of grain size change (as indicated by the nearly vertical contour lines in Figure 8). This relation is consistent with the observation that the majority of the total grain size change caused by RoR development occurs within the first year following the supply disruption (assuming a normal duration of bed load transporting flows during the first year).

While high sediment supply channels are susceptible to substantial changes in grain size, these channels also have fast recovery times once supply is reestablished (Figure 5). Based on our selection of model input parameters, which reflect conditions of Pacific Northwest and British Columbia streams, the recovery time for high sediment supply channels can be less than 1 year. For low sediment supply channels, the recovery time can be as long as a decade, but the impact is so minor from a geomorphological perspective that the changes in surface grain size are negligible.

We have assumed that the diversion reach passes sediment without acting as a storage element. The boundary shear stress in the diversion reach at bankfull flows is 6–13 times the critical value used in the Parker [1990] model assuming a slope of 0.1 and 3–7 times the critical value assuming a slope of 0.04. It is unlikely that there can be significant sediment deposition with flows of this magnitude. Nevertheless, there will be a time lag between dam closure and disruption of sediment supply to the downstream reach that depends on the length of the diversion reach and the number of bed load transporting flows passed through the diversion reach following dam closure. During this time lag, sediment within the diversion reach prior to dam closure will continue to supply the downstream reach during flood flows (as will any sediment delivered directly to the diversion reach via hillslopes or tributary junctions). It is difficult to estimate the magnitude of this time lag without knowing the virtual velocity of sediment in the diversion reach.

In our analysis of model results, we focus on the grain size response because the availability and size distribution of gravel is known to impact salmon spawning and could ultimately affect salmon population dynamics [Kondolf *et al.*, 1996; Ligon *et al.*, 1995]. The magnitude of grain size change predicted by the model can impact the suitability of the channel for anadromous Pacific salmon (*Oncorhynchus* sp.). For example, in the high sediment supply, gravel bed scenario (Figure 5a), the preproject channel is suitable for Chinook (*O. tshawytscha*), Chum (*O. keta*), Pink (*O. gorbuscha*), and Sockeye (*O. nerka*) salmon [Riebe *et al.*, 2014; Kondolf and Wolman, 1993] (adequate data were not available for Coho and Steelhead species). Following supply disruption to the downstream reach, however, the change in grain size is large enough to shift the  $D_{50}$  out of the range suitable for Sockeye, Chum, and possibly Pink salmon. The grain size change is not large enough, however, to shift the  $D_{50}$  out of the range suitable for Chinook salmon. Results are similar for the coarse gravel channel (Figure 5b) where the preproject grain size is suitable for Chinook and Pink salmon. Following the disruption of sediment supply to the downstream reach, however, the change in grain size is substantial enough to shift the  $D_{50}$  out of the range suitable for Chinook and Pink salmon. Depending on the size of the head-pond and duration of the supply disruption, these grain size changes could exist for several years.

Extending these results to the annual lifecycle of anadromous Pacific salmon (*Oncorhynchus* sp.), short-term (<1 year) changes to sediment size that occur inside the spawning and embryonic incubation periods (usually Summer–Spring) are expected to have moderate to high potential impact on spawning and productivity in that year, but such effects are expected to be transient and impacts on long-term population productivity minimal. In contrast, sediment size distributions that are altered for one or more years (as in the case of the large head-pond scenarios in Figure 5) have the potential to affect multiple generations of spawning anadromous salmon, and therefore emergent population dynamics. While we recognize that bed surface grain size is not the only variable that determines the suitability of spawning habitat, our modeling does suggest that a substantial change in grain size can occur and that it has the potential to adversely affect salmon spawning habitat.

Because we have treated the head-pond as the sole storage element in our modeling scenarios, our results could underestimate the grain size impacts. Although the diversion reach has limited storage capacity and is subject to sediment-transporting flows during flood events, reduced flows during most of the year could increase sediment storage within the diversion reach, increasing the opportunity for chronic long-term sediment storage and supply reduction to the downstream reach. We have also assumed the head-pond is a perfectly efficient sediment trap, meaning all supplied sediment is trapped. It is more likely that the coarsest

particles in the supply distribution are preferentially trapped, causing the GSD of bed load material passed by the dam to become finer. This can result in fining of sediment in both the diversion reach and the downstream reach, which could have very different impacts to the ecological function of these reaches. Understanding the effect of a change in the grain size distribution delivered to the downstream reach following reestablishment of sediment supply is important to further our understanding of potential impacts. But before this can be done, field data are needed that show how the grain size distribution leaving the head-pond changes once the dead-storage volume is full.

Nevertheless, our results do provide some guidance to anticipate the sediment supply conditions and head-pond sizes that are apt to cause significant grain size change. The challenge in applying these results is estimating the bed load supply to channels. There has been some work that links sediment supply to bed armor ratios [Dietrich *et al.*, 1989], bed surface grain size to sediment supply [Buffington and Montgomery, 1999], and sediment yield to both the size and volume of fine sediment in pools [Lisle and Hilton, 1999]. However, these relations have not been widely tested. As such there is no generally accepted way to evaluate the sediment supplied to rivers. There is a need to develop regionally applicable relations between sediment supply and basin characteristics suitable for application to channels where RoR projects are being located.

Our simulations confirm what a knowledgeable geomorphologist would qualitatively predict about how gravel bed channel surfaces would respond to variations in sediment supply. But our method provides objective, quantitative estimates that may be used in assessing potential future impact of RoR development. This provides an alternative methodology to estimating impacts by postproject monitoring. At present, required monitoring of RoR projects is not detailed enough to provide meaningful data to interpret geomorphological impacts given the spatial and temporal variability in sediment supply to fluvial systems. Our methodology should not be used to supplant routine monitoring of geomorphic impacts of RoR projects, however the modeling allows for development of testable hypotheses that targeted monitoring can assess.

## 6. Conclusions

An increase in the rate of RoR development in British Columbia and other parts of the world (e.g., China and India) has eclipsed our understanding of their potential environmental impact. While perceived as low-impact, that perception has never been quantitatively tested. Long-term field monitoring has been the only way to better understand the impacts of RoR development. However, given the increased rate of development and the time required before impacts are detectable in the field, the impacts of RoR dams may be fully manifest before they are well understood. To better understand the geomorphic impacts of RoR development before they emerge, we modeled impacts on grain size due to likely sediment disruption scenarios associated with development of high-head projects on steep mountain channels. Using a 1-D morphodynamic model and some limited field observations, we modeled a range of sediment disruption scenarios using field data from three different RoR sites in British Columbia. By varying the preproject bed load supply rate and the time scale over which supply is disrupted, we produce a matrix of predicted change in surface grain size as a function of these two variables.

Our model results lead to the following conclusions:

1. Morphodynamic modeling of a temporary sediment supply disruption associated with run-of-river hydropower development indicates changes in bed-surface grain size can range from substantial (74% increase in surface  $D_{50}$ ) to negligible (1% increase in the surface  $D_{50}$ ) in the downstream reach depending primarily on the predevelopment bed load supply rate and secondarily on the time scale of disruption;
2. The greatest change in the median surface grain size is predicted to occur at sites where the predevelopment sediment supply rate is high and for projects with substantial sediment storage capacity within their head-ponds;
3. Grain size impacts are negligible for project sites with low predevelopment sediment supply;
4. The recovery time for a channel to reestablish the predevelopment surface  $D_{50}$  appears to be inversely related to the predevelopment sediment supply rate such that channels with high predevelopment sediment supply have short recovery times;

5. The short-term impact of RoR development on salmon spawning habitat in the downstream reach is likely to be greatest, in terms of magnitude of grain size change, in channels with relatively high predevelopment sediment supply. The impact will depend on the predevelopment surface grain size distribution and the species present in the channel.

Application of our results or this modeling technique to the RoR site selection process requires the ability to calculate reasonable estimates of bed load supply. The lack of such relations for many regions represents a major challenge to predicting the impacts of run-of-river development. Development of regional bed load supply curves would greatly enhance the ability of morphodynamic models to predict the geomorphic impacts of RoR development. Regular surveys of head-pond deposition at existing RoR facilities would greatly enhance the ability to develop accurate regional bed load supply curves. Future research is also necessary for predicting the downstream extent of the grain size impacts identified here.

### Acknowledgments

The research was funded by a grant from the Gordon and Betty Moore Foundation to W.J.P. The authors wish to thank Viorel Popescu for many helpful and informative discussions with the lead author. Thoughtful reviews from Rob Ferguson and two anonymous reviewers improved the quality of this manuscript as did reviews from Tom Lisle, Jim Pizzuto, and Mike Church on an earlier draft. Discussions with Northwest Hydraulics Consultants, Knight-Piesold, and Innergex Renewable Energy Inc. helped us better understand design, operation, and potential impacts of RoR hydro projects. Matt Akenhead played a vital role in the collection of field data that were used as input to the model. All data presented in this paper are freely available from the corresponding author.

### References

- Abbasi, T., and S. A. Abbasi (2011), Small hydro and the environmental implications of its extensive utilization, *Renewable Sustainable Energy Rev.*, 15(4), 2134–2143, doi:10.1016/j.rser.2010.11.050.
- Allred, T. M., and J. C. Schmidt (1999), Channel narrowing by vertical accretion along the Green River near Green River, Utah, *Geol. Soc. Am. Bull.*, 111, 1757–1772, doi:10.1130/0016-7606(1999)111<1757:CNBVAA>2.3.CO;2.
- Anderson, D., H. Moggridge, P. Warren, and J. Shucksmith (2014), The impacts of 'run-of-river' hydropower on the physical and ecological condition of rivers, *Water Environ. J.*, 29, 268–276, doi:10.1111/wej.12101.
- Andrews, E. (1980), Effective and bankfull discharges of streams in the Yampa River Basin, Colorado and Wyoming, *J. Hydrol.*, 46(3–4), 311–330, doi:10.1016/0022-1694(80)90084-0.
- Andrews, E. D. (1986), Downstream effects of Flaming Gorge Reservoir on the Green River, Colorado and Utah, *Geol. Soc. Am. Bull.*, 97, 1012–1023, doi:10.1130/0016-7606(1986)97<1012:DEOFGR>2.0.CO;2.
- Baker, D. W., B. P. Bledsoe, C. M. Albano, and N. L. Poff (2011), Downstream effects of diversion dams on sediment and hydraulic conditions of rocky mountain streams, *River Res. Appl.*, 27(3), 388–401, doi:10.1002/rra.1376.
- Buffington, J., and D. Montgomery (1999), Effects of sediment supply on surface textures of gravel-bed rivers, *Water Resour. Res.*, 35(11), 3523–3530, doi:10.1029/1999WR900232.
- Bunte, K., and S. R. Abt (2001), Sampling surface and subsurface particle-size distributions in wadable gravel-and cobble-bed streams for analyses in sediment transport, hydraulics, and streambed monitoring, *Gen. Tech. Rep. RMRS-GTR-74*, U.S. Dep. of Agric., Fort Collins, Colo.
- Church, M. (1992), Channel morphology and typology, in *The Rivers Handbook*, edited by P. Calow and G. E. Petts, pp. 126–143, Blackwell Sci., Oxford, U. K.
- Church, M. (2006), Bed material transport and the morphology of alluvial river channels, *Annu. Rev. Earth Planet. Sci.*, 34, 325–354.
- Cloudworks Energy Inc. (2011), *Tretheway Creek Waterpower Project, Shovel Creek Waterpower Project, Big Silver Waterpower Project, Application for an Environmental Assessment Certificate*, B. C. Environ. Assess. Off. – Proj. Inf. Cent. (e-PIC), Vancouver, B. C., Canada. [Available at [http://a100.gov.bc.ca/appsdata/epic/html/deploy/epic\\_project\\_list\\_report.html](http://a100.gov.bc.ca/appsdata/epic/html/deploy/epic_project_list_report.html).]
- Creek Power (2012), *Upper Lillooet Hydro Project, Environmental Assessment Certificate Application*, B. C. Environ. Assess. Off.–Proj. Inf. Cent. (e-PIC), Vancouver, B. C., Canada. [Available at [http://a100.gov.bc.ca/appsdata/epic/html/deploy/epic\\_project\\_list\\_report.html](http://a100.gov.bc.ca/appsdata/epic/html/deploy/epic_project_list_report.html).]
- Csiki, S. J. C., and B. L. Rhoads (2014), Influence of four run-of-river dams on channel morphology and sediment characteristics in Illinois, USA, *Geomorphology*, 206, 215–229, doi:10.1016/j.geomorph.2013.10.009.
- Cui, Y., and G. Parker (2005), Numerical model of sediment pulses and sediment-supply disturbances in mountain rivers, *J. Hydraul. Eng.*, 131, 646–656.
- Cui, Y., C. Paola, and G. Parker (1996), Numerical simulation of aggradation and downstream fining, *J. Hydraul. Res.*, 34(2), 185–204.
- Cui, Y., G. Parker, J. Pizzuto, and T. E. Lisle (2003), Sediment pulses in mountain rivers: 2. Comparison between experiments and numerical predictions, *Water Resour. Res.*, 39(9), 1240, doi:10.1029/2002WR001805.
- Cui, Y., G. Parker, C. Braudrick, W. E. Dietrich, and B. Cluer (2006a), Dam Removal Express Assessment Models (DREAM) Part 1: Model development and validation, *J. Hydraul. Res.*, 44(3), 291–307.
- Cui, Y., C. Braudrick, W. E. Dietrich, B. Cluer, and G. Parker (2006b), Dam Removal Express Assessment Models (DREAM) Part 2: Sample runs/sensitivity tests, *J. Hydraul. Res.*, 44(3), 308–323.
- Cui, Y., J. Wooster, J. Venditti, S. Dusterhoff, W. Dietrich, and L. Sklar (2008), Simulating sediment transport in a flume with forced pool-riffle morphology: Examinations of two one-dimensional numerical models, *J. Hydraul. Eng.*, 134(7), 892–904.
- Dietrich W., J. Kirchner, H. Ikeda, and F. Iseya (1989), Sediment supply and the development of the coarse surface-layer in gravel-bedded rivers, *Nature*, 340(6230), 215–217, doi:10.1038/340215a0.
- Dudhani, S., A. K. Sinha, and S. S. Inamdar (2006), Assessment of small hydropower potential using remote sensing data for sustainable development in India, *Energy Policy*, 34(17), 3195–3205.
- Endreny, T. A. (2007), Estimation of channel bankfull occurrence from instantaneous discharge data, *J. Hydrol. Eng.*, 12(5), 524–531, doi:10.1061/(ASCE)1084-0699(2007)12(5)524.
- Ferguson, R., (2007), Flow resistance equations for gravel-and boulder-bed streams, *Water Resour. Res.*, 43, W05427, doi:10.1029/2006WR005422.
- Ferguson, R. I., and M. Church (2009), A critical perspective on 1-D modeling of river processes: Gravel load and aggradation in lower Fraser River, *Water Resour. Res.*, 45, W11424, doi:10.1029/2009WR007740.
- Ferguson, R. I., M. Church, C. D. Rennie, and J. G. Venditti (2015), Reconstructing a sediment pulse: Modeling the effect of placer mining on Fraser River, Canada, *J. Geophys. Res. Earth Surf.*, 120, 1436–1454, doi:10.1002/2015JF003491.
- Friedman, J. M., W. R. Osterkamp, and W. M. Lewis (1996a), The role of vegetation and bed-level fluctuations in the process of channel narrowing, *Geomorphology*, 14, 341–351, doi:10.1016/0169-555X(95)00047-9.

- Friedman, J. M., W. R. Osterkamp, and W. M. Lewis (1996b), Channel narrowing and vegetation development following a Great Plains flood, *Ecology*, *77*, 2167–2181, doi:10.2307/2265710.
- Graf, W. L. (1978), Fluvial adjustments to the spread of tamarisk in the Colorado Plateau region, *Geol. Soc. Am. Bull.*, *89*, 1491–1501, doi:10.1130/0016-7606(1978)89<1491:FATTSO>2.0.CO;2.
- Grams, P. E., and J. C. Schmidt (2002), Streamflow regulation and multilevel flood plain formation: Channel narrowing on the aggrading Green River in the eastern Uinta Mountains, Colorado and Utah, *Geomorphology*, *44*, 337–360, doi:10.1016/S0169-555X(01)00182-9.
- Grams, P. E., and J. C. Schmidt (2005), Equilibrium or indeterminate? Where sediment budgets fail: Sediment mass balance and adjustment of channel form, Green River downstream from Flaming Gorge Dam, Utah and Colorado, *Geomorphology*, *71*, 156–181, doi:10.1016/j.geomorph.2004.10.012.
- Grant, G. (2012), The geomorphic response of gravel-bed rivers to dams: Perspectives and prospects, in *Gravel-Bed Rivers: Processes, Tools, Environments*, edited by M. Church, P. M. Biron, and G. Roy, John Wiley & Sons, Ltd., Chichester, U. K., doi:10.1002/9781119952497.ch15.
- Guégan, J. F., S. Lek, and T. Oberdorff (1998), Energy availability and habitat heterogeneity predict global riverine fish diversity, *Nature*, *391*(6665), 382–384.
- Harrison, A. S. (1950), *Report on Special Investigation of Bed Sediment Segregation in a Degrading Bed*, vol. 1, series 33, issue 1, 205 pp., Univ. of Calif., Inst. of Eng. Res., Berkeley.
- Hassan, M. A., D. Brayshaw, Y. Alila, and E. Andrews (2014), Effective discharge in small formerly glaciated mountain streams of British Columbia: Limitations and implications, *Water Resour. Res.*, *50*, 4440–4458, doi:10.1002/2013WR014529.
- Hoey, T. B., and R. Ferguson (1994), Numerical simulation of downstream fining by selective transport in gravel bed rivers: Model development and illustration, *Water Resour. Res.*, *30*(7), 2251–2260, doi:10.1029/94WR00556.
- Jaccard, M., N. Melton, and J. Nyboer (2011), Institutions and processes for scaling up renewables: Run-of-river hydropower in British Columbia, *Energy Policy*, *39*(7), 4042–4050, doi:10.1016/j.enpol.2011.02.035.
- Kerr, J. T., and L. Packer (1997), Habitat heterogeneity as a determinant of mammal species richness in high energy regions, *Nature*, *385*, 252–254.
- Kibler, K. M., and D. D. Tullis (2013), Cumulative biophysical impact of small and large hydropower development in Nu River, China, *Water Resour. Res.*, *49*, 3104–3118, doi:10.1002/wrcr.20243.
- Knighton, D. (1988), The impact of Parangana Dam on the River Mersey, Tasmania, *Geomorphology*, *1*, 221–237, doi:10.1016/0169-555X(88)90015-3.
- Knight Piesold Ltd. (2008), *Upper Toba Valley Hydroelectric Project, Environmental Assessment Certificate Application*, B. C. Environ. Assess. Off.–Proj. Inf. Cent. (e-PIC), Vancouver, B. C., Canada. [Available at [http://a100.gov.bc.ca/appsdata/epic/html/deploy/epic\\_project\\_list\\_report.html](http://a100.gov.bc.ca/appsdata/epic/html/deploy/epic_project_list_report.html).]
- Kondolf, G., and M. Wolman (1993), The Sizes of Salmonid Spawning Gravels, *Water Resour. Res.*, *29*(7), 2275–2285, doi:10.1029/93WR00402.
- Kondolf, G. M. (1997), Hungry water: Effects of dams and gravel mining on river channels, *Environ. Manage.*, *21*(4), 533–551.
- Kondolf, G. M., and W. V. Matthews (1991), *Management of Coarse Sediment in Regulated Rivers of California*, Univ. of Calif. Water Resour. Cent, Berkeley, Calif.
- Kondolf, G. M., J. C. Vick, and T. M. Ramirez (1996), Salmon spawning habitat rehabilitation on the Merced River, California: An evaluation of project planning and performance, *Trans. Am. Fish. Soc.*, *125*(6), 899–912.
- Kuhnle, R., and J. Southard (1988), Bed-load transport fluctuations in a gravel bed laboratory channel, *Water Resour. Res.*, *24*(2), 247–260, doi:10.1029/WR024i002p00247.
- Lenzi, M. A., L. Mao, and F. Comiti (2006), Effective discharge for sediment transport in a mountain river: Computational approaches and geomorphic effectiveness, *J. Hydrol.*, *326*(1), 257–276.
- Ligon, F., W. Dietrich, and W. Trush (1995), Downstream ecological effects of dams, *Bioscience*, *45*(3), 183–192, doi:10.2307/1312557.
- Lisle, T., F. Iseya, and H. Ikeda (1993), Response of a channel with alternate bars to a decrease in supply of mixed-size bed-load—A flume experiment, *Water Resour. Res.*, *29*(11), 3623–3629, doi:10.1029/93WR01673.
- Lisle, T. E. (1995), Particle size variations between bed load and bed material in natural gravel bed channels, *Water Resour. Res.*, *31*(4), 1107–1118.
- Lisle, T. E., and S. Hilton (1999), Fine bed material in pools of natural gravel bed channels, *Water Resour. Res.*, *35*(4), 1291–1304.
- Lisle, T. E., J. M. Nelson, J. Pitlick, M. A. Madej, and B. L. Barkett (2000), Variability of bed mobility in natural gravel-bed channels and adjustments to sediment load at the local and reach scales, *Water Resour. Res.*, *36*(12), 3743–3756.
- MacArthur, R. H., and J. W. MacArthur (1961), On bird species diversity, *Ecology*, *42*, 594–598.
- Merritt, D. M., and D. J. Cooper (2000), Riparian vegetation and channel change in response to river regulation: A comparative study of regulated and unregulated streams in the Green River Basin, USA, *Reg. Rivers Res. Manage.*, *16*, 543–564, doi:10.1002/1099-1646(200011/12)16:6<543::AID-RRR590>3.0.CO;2-N
- Montgomery, D. R., and J. M. Buffington (1997), Channel-reach morphology in mountain drainage basins, *Geol. Soc. Am. Bull.*, *109*(5), 596–611.
- Nelson, P. A., J. G. Venditti, W. E. Dietrich, J. W. Kirchner, H. Ikeda, F. Iseya, and L. S. Sklar (2009), Response of bed surface patchiness to reductions in sediment supply, *J. Geophys. Res.*, *114*, F02005, doi:10.1029/2008JF001144.
- Palmer, M. A., H. L. Menninger, and E. Bernhardt (2009), River restoration, habitat heterogeneity and biodiversity: A failure of theory or practice?, *Freshwater Biol.*, *55*(S1), 205–222.
- Parker, G. (1991), Selective sorting and abrasion of river gravel. I: Theory, *J. Hydraul. Eng.*, *117*(2), 131–147.
- Parker, G. (1990), Surface-based bedload transport relation for gravel rivers, *J. Hydraul. Res.*, *28*(4), 417–436.
- Parker, G. (2004), 1D sediment transport morphodynamics with applications to rivers and turbidity currents [electronic], St. Anthony Falls Laboratory, Minneapolis, Minn. [Available at [http://hydrolab.illinois.edu/people/parkerg//morphodynamics\\_e-book.htm](http://hydrolab.illinois.edu/people/parkerg//morphodynamics_e-book.htm).]
- Parker, G. (2008), Chapter 3: Transport of gravel and sediment mixtures, in *Sedimentation Engineering: Theories, Measurements, Modeling and Practice*, ASCE Manual and Reports on Engineering Practice, vol. 110, edited by M. H. Garcia, pp. 165–264, Am. Soc. of Civ. Eng., Reston, Va.
- Parker, G., and P. Klingeman (1982), On why gravel bed streams are paved, *Water Resour. Res.*, *18*(5), 1409–1423, doi:10.1029/WR018i005p01409.
- Parker, G., and C. Toro-Escobar (2002), Equal mobility of gravel in streams: The remains of the day, *Water Resour. Res.*, *38*(11), 1264, doi:10.1029/2001WR000669.
- Parker, G., M. Hassan, and P. Wilcock (2007), Adjustment of the bed surface size distribution of gravel-bed rivers in response to cycled hydrographs, *Dev. Earth Surf. Processes*, *11*, 241–285.



- Pelpola, C., and E. Hickin (2004), Long-term bed load transport rate based on aerial-photo and ground penetrating radar surveys of fan-delta growth, Coast Mountains, British Columbia, *Geomorphology*, *57*(3–4), 169–181, doi:10.1016/S0169-555X(03)00101-6.
- Podolak, C. J., and P. R. Wilcock (2013), Experimental study of the response of a gravel streambed to increased sediment supply, *Earth Surf. Process. Landforms* *38*, 1748–1764, doi:10.1002/esp.3468.
- Purohit, P. (2008), Small hydro power projects under clean development mechanism in India: A preliminary assessment, *Energy Policy*, *36*(6), 2000–2015.
- Ray, D. (2011), *Tretheway Creek, Shovel Creek and Big Silver Creek Waterpower Projects, Overview-level Geomorphic Assessment, Appendix N, Application for an Environmental Assessment Certificate*, B. C. Environ. Assess. Off.–Proj. Inf. Cent, Vancouver, B. C., Canada. [Available at [http://a100.gov.bc.ca/appsdata/epic/html/depoy/epic\\_document\\_325\\_33955.html](http://a100.gov.bc.ca/appsdata/epic/html/depoy/epic_document_325_33955.html).]
- Rickenmann, D., and A. Recking (2011), Evaluation of flow resistance in gravel-bed rivers through a large field data set, *Water Resour. Res.*, *47*, W07538, doi:10.1029/2010WR009793.
- Riebe, C. S., L. S. Sklar, B. T. Overstreet, and J. K. Wooster (2014), Optimal reproduction in salmon spawning substrates linked to grain size and fish length, *Water Resour. Res.*, *50*, 898–918.
- Skalak, K., J. Pizzuto, and D. D. Hart (2009), Influence of small dams on downstream channel characteristics in Pennsylvania and Maryland: Implications for the long-term geomorphic effects of dam removal, *J. Am. Water Resour. Assoc.*, *45*(1), 97–109, doi:10.1111/j.1752-1688.2008.00263.x.
- Tews J., U. Brose, V. Grimm, K. Tielbörger, M. C. Wichmann, M. Schwager, and F. Jeltsch (2004), Animal species diversity driven by habitat heterogeneity-diversity: The importance of keystone structures, *J. Biogeogr.*, *31*, 79–92.
- Venditti, J. G., W. E. Dietrich, P. A. Nelson, M. A. Wydzga, J. Fadde, and L. Sklar (2010), Effect of sediment pulse grain size on sediment transport rates and bed mobility in gravel bed rivers, *J. Geophys. Res.*, *115*, F03039, doi:10.1029/2009JF001418.
- Venditti, J. G., P. A. Nelson, J. T. Minear, J. Wooster, and W. E. Dietrich (2012), Alternate bar response to sediment supply termination, *J. Geophys. Res.*, *117*, F02039, doi:10.1029/2011JF002254.
- Viparelli, E., O. E. Sequeiros, A. Cantelli, P. R. Wilcock, and G. Parker (2010), River morphodynamics with creation/consumption of grain size stratigraphy. 2: Numerical model, *J. Hydraul. Res.*, *48*(6), 727–741.
- Viparelli, E., D. Gaeuman, P. Wilcock, and G. Parker (2011), A model to predict the evolution of a gravel bed river under an imposed cyclic hydrograph and its application to the Trinity River, *Water Resour. Res.*, *47*, W02533, doi:10.1029/2010WR009164.
- Wampler, P. (2004), Contrasting geomorphic responses to climatic, anthropogenic, and fluvial change across modern to millennial time scales, Clackamas River, Oregon, PhD thesis, Dep. of Geosci., Oreg. State Univ., Corvallis.
- Whiting, P. J., and J. G. King (2003), Surface particle sizes on armoured gravel streambeds: Effects of supply and hydraulics, *Earth Surf. Processes Landforms*, *28*(13), 1459–1471.
- Wilcock, P. R., and J. C. Crowe (2003), Surface-based transport model for mixed-size sediment, *J. Hydraul. Eng.*, *129*(2), 120–128.
- Williams, G. P., and M. G. Wolman (1984), Downstream effects of dams on alluvial rivers, *U. S. Geol. Surv. Geol. Surv. Prof. Pap.*, *1286*, pp. 1–83, Washington, D. C.
- Yager, E. M., J. W. Kirchner, and W. E. Dietrich (2007), Calculating bed load transport in steep boulder bed channels, *Water Resour. Res.*, *43*, W07418, doi:10.1029/2006WR005432.
- Zhou, S., X. Zhang, and J. Liu (2009), The trend of small hydropower development in China, *Renewable Energy*, *34*(4), 1078–1083.